NOAA Technical Memorandum ERL AOML-14

U.S. DEPARTMENT OF COMMERCE
NATIONAL OCEANIC AND ATMOSPHERIC ADMINISTRATION
Environmental Research Laboratories

Free-Air Gravity Anomalies South of Panama and Costa Rica (NOAA Ship OCEANOGRAPHER - August 1969)

ROBERT J. BARDAY

Atlantic
Oceanographic
and
Meteorological
Laboratories
MIAMI
FLORIDA
September 1971

ENVIRONMENTAL RESEARCH LABORATORIES

ATLANTIC OCEANOGRAPHIC AND METEOROLOGICAL LABORATORIES

NATIONAL OCEANIC AND ATMOSPHERIC ADMINISTRATION

U.S. DEPARTMENT OF COMMERCE
National Oceanic and Atmospheric Administration
Environmental Research Laboratories

NOAA Technical Memorandum ERL AOML-14

FREE-AIR GRAVITY ANOMALIES SOUTH OF PANAMA AND COSTA RICA (NOAA SHIP OCEANOGRAPHER - AUGUST 1969)

Robert J. Barday

Marine Geology and Geophysics Laboratory

Atlantic Oceanographic and Meteorological Laboratories
Miami, Florida
September 1971

TABLE OF CONTENTS

ILLUSTRATIONS

FREE-AIR GRAVITY ANOMALIES SOUTH OF PANAMA AND COSTA RICA

(NOAA SHIP OCEANOGRAPHER - August 1969)

Robert J. Barday

Free-air anomaly profiles from a geophysical investigation centered on the Panama Fracture Zone are presented with their corresponding bathymetric profiles. The quality of these profiles is indicated by a mean free-air anomaly discrepancy of 3.48 milligals with a standard deviation of 3.28 milligals for 99 crossings of the ship's track. These data support the existence of a deep, sediment-filled depression at the northern end of the Panama Fracture Zone, the presence of a sediment-filled marginal trough east of the Coiba Ridge, and the accumulation of thick sedimentary deposits on the eastern flanks of both the Cocos and Coiba Ridges. The gravity data also suggest that there is no large-scale change in crustal structure across the Panama Fracture Zone, and the entire survey area may be slightly out of isostatic adjustment.

1. INTRODUCTION

In August 1969 a geophysical investigation of the Panama Fracture Zone was conducted by the National Oceanic and Atmospheric Administration Ship OCEANOGRAPHER. Depth, total magnetic intensity, and gravity meter readings were recorded continuously over approximately 11,200 km of track-line controlled by satellite navigation. This report presents free-air anomaly profiles and discusses certain

geological conclusions that are consistent with the observed gravity data.

2. DATA ACQUISITION AND REDUCTION

By definition, the free-air anomaly can be expressed as

$$FA=g_o-\gamma_o \tag{1}$$

where $\gamma_o=978.049(1+0.0052884\sin^2\phi-0.0000059\sin^2 2\phi)$ is the theoretical sea level gravity given by the 1930 international gravity formula, and g_o is the observed gravity reduced to sea level. For sea level gravity observations

$$g_o=ZMG+R+E_c+D_c \tag{2}$$

where ZMG (zeroed meter gravity) is a value equivalent to a gravity meter reading of zero, R is the meter reading (in milligals), E_c is the Eötvös correction, and D_c is the drift correction.

Both data acquisition and reduction can most easily be discussed from a term-by-term consideration of (2).

2.1 Zeroed Meter Gravity

The ZMG was obtained from a land tie at Rodman Naval Station, Canal Zone, immediately before the survey. [The details of the ZMG computation have been discussed by Orlin and Sibila (1966).] The base station is described by Woollard and Rose (1963) as follows:

WH 1015. Rodman Naval Base, at shore end of center of three piers next to large valve block painted black and yellow, Lamont No. BE 1-1.

2.2 Gravity Meter Reading

The gravity meter used for this survey was Askania "Sea Gravimeter Gss2 after Graf', Model C, No. 22 (Graf and Schulze, 1961; Schulze, 1962) mounted on an electrically erected Anschütz Gyrotable. The gravity meter dial reading, R_d ($R_d=R/K_d$ where K_d is a constant necessary to convert dial divisions into milligals), was recorded both digitally and on analog strip chart.

All digitized dial readings were plotted against time, and the values appearing to be inconsistent were checked against the analog strip chart. If discrepancies were found, the digitized values were adjusted. If the inconsistencies persisted, the values in question were deleted unless they could be related to any changes in speed or changes in course less than 90°.

2.3 Eötvös Correction

Accurate navigation is critical to marine gravity observations. At 5°N, the mean latitude of this survey, and at 27 km/hr, the average speed of this survey, the rates at

which the Eötvös correction changes with respect to course and speed are 2.1 milligals/° (for a N-S trackline) and 3.7 milligals/km/hr (for an E-W trackline). If the free-air anomaly is to be determined to an accuracy of 1 milligal (the accuracy to which R was measured), the course and speed must be known within 0.5° and 0.2 km/hr, respectively.

Because the course and speed are computed from the smooth plotted track, their accuracy depends upon the accuracy of the fixes, the elapsed time between fixes, and the interpolation method used to determine the ship's track between fixes.

This survey was controlled by the Navy's satellite navigation system with the AN/SRN-9 equipment (Guier, 1966). The accuracy of this system is largely influenced by uncertainty in the ship's velocity. As a first approximation, a 1.8-km/hr error in the ship's velocity results in a 0.45-km error in the computed satellite fix (Stansell, 1970). If the velocity is estimated from sea trial data or the speed made good between previous fixes, as in the case of this survey, then the computed fixes may be in error by as much as 2 km.

The average time interval between fixes was 2 hr. At this interval an error of 45 km in the satellite fixes would result in a one-milligal error in the computed Eötvös

correction. However, the elapsed time between fixes ranged downward to 22 minutes implying a possible error in the Eötvös correction of 10 milligals or more.

The interpolation method used to determine the smooth plotted track was based on the assumption that the course and speed made good are constant between navigation points. (Navigation point is used here to mean a point where there is a satellite fix or a change in course and/or speed.) The computed Eötvös correction was, therefore, a discontinuous step function rather than a continuous function between course and speed changes.

To remove these artificial discontinuities and minimize error in the Eötvös correction, the following technique was used (refer to fig. 1):

(1) For all but E-W lines both the speed made good, SMG (B, fig. 1), and the difference between the course made good and the course steered, CMG-CST (A, fig. 1), were plotted against time. Both plots were then approximated by piecewise continuous curves in which discontinuities occurred at any changes in speed and at changes in course greater than 10°.

(2) For E-W lines the Eötvös correction (C, fig. 1), rather than SMG and CMG-CST, was similarly treated.

(3) These piecewise continuous curves were, in turn, approximated by straight line segments.

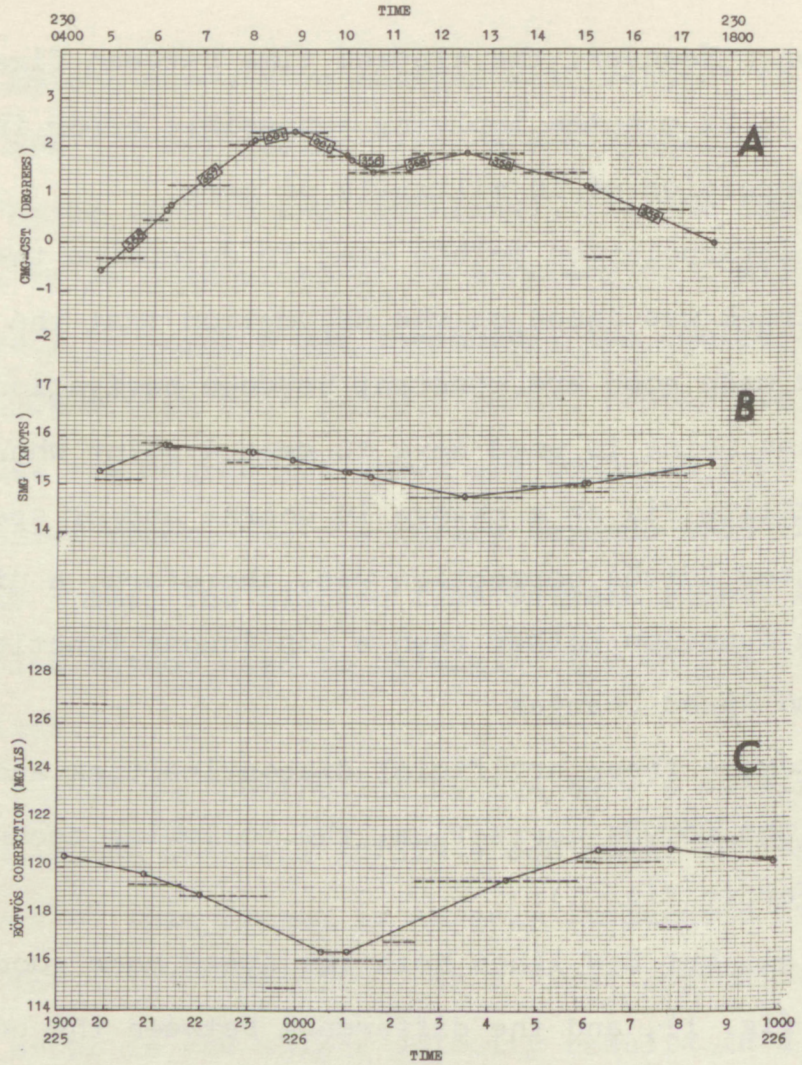

Figure 1. Based on the assumption that the course and speed made good are constant between navigation points, the difference between the course made good and the course steered (CMG-CST), the speed made good (SMG), and the Eötvös correction become piecewise continuous step functions of time [dashed curves (---)]. The solid curves (___) illustrate a technique whereby these parameters can be made to more closely approximate continuous functions of time (not shown for clarity). Curves A and B are from a N-S profile (No. 14) and curve C is from an E-W profile (No. 3). The numbers enclosed in boxes (359) signify the course steered for each segment of the CMG-CST curve bounded by circles (o). The Eötvös correction used to compute the free-air anomaly is determined from a linear time interpolation of the circled values.

(4) The time, course, and speed or the time and Eötvös correction at each break in slope were entered into a computer program that obtained the free-air anomaly at each data point using the Eötvös correction computed from a linear time interpolation of these parameters. For all but E-W lines the program also requires course and speed values immediately before and after each change in course steered.

This technique is based on the assumption that the difference between the course and speed made good and the ordered course and speed is the result of the current acting on the ship. Although current in this sense of the word includes many factors in addition to horizontal movement of the water, its effect on the ship should vary smoothly between large changes in course and speed. Therefore, the speed made good and the difference between the course made good and the course steered should be continuous functions of time between speed changes and large changes in course steered. Because the Eötvös correction computed for E-W lines is insensitive to small changes in course, it must likewise be continuous.

2.4 Drift Correction

Because of instrumentation failure it was impossible to complete a land tie at the conclusion of this survey. The drift, D [$D=-D_c/(t-t_o)$ where t is the time of observation and t_o is the time of ZMG determination], was determined as follows:

(1) The free-air anomaly was computed without a drift correction.

(2) The differences ΔFA_{ij} and Δt_{ij} where $i<j$ were determined for each trackline intersection; $\Delta FA_{ij}=FA_{ji}-FA_{ij}$ and $\Delta t_{ij}=t_{ji}-t_{ij}$ where FA_{ji} is the free-air anomaly and t_{ji} is the time of profile j at its intersection with profile i.

(3) The drift was computed by a least squares fit of the function $\Delta FA=D\times\Delta t$ to the pairs $\Delta FA_{ij},\Delta t_{ij}$.

Illustrated in figure 2, this procedure follows from the identities $FAN_{ij}\equiv FA_{ij}-D\times(t_{ij}-t_o)$ and $FAN_{ji}\equiv FA_{ji}-D\times(t_{ji}-t_o)$ where FAN_{ji} is the drift-corrected free-air anomaly of profile j at its intersection with profile i. Therefore,

$$\begin{aligned}\Delta FAN_{ij} &= FAN_{ji}-FAN_{ij}\\ &= FA_{ji}-D\times(t_{ji}-t_o)-FA_{ij}+D\times(t_{ij}-t_o)\\ &= FA_{ji}-FA_{ij}-D\times(t_{ji}-t_{ij})\\ &= \Delta FA_{ij}-D\times\Delta t_{ij}.\end{aligned}$$

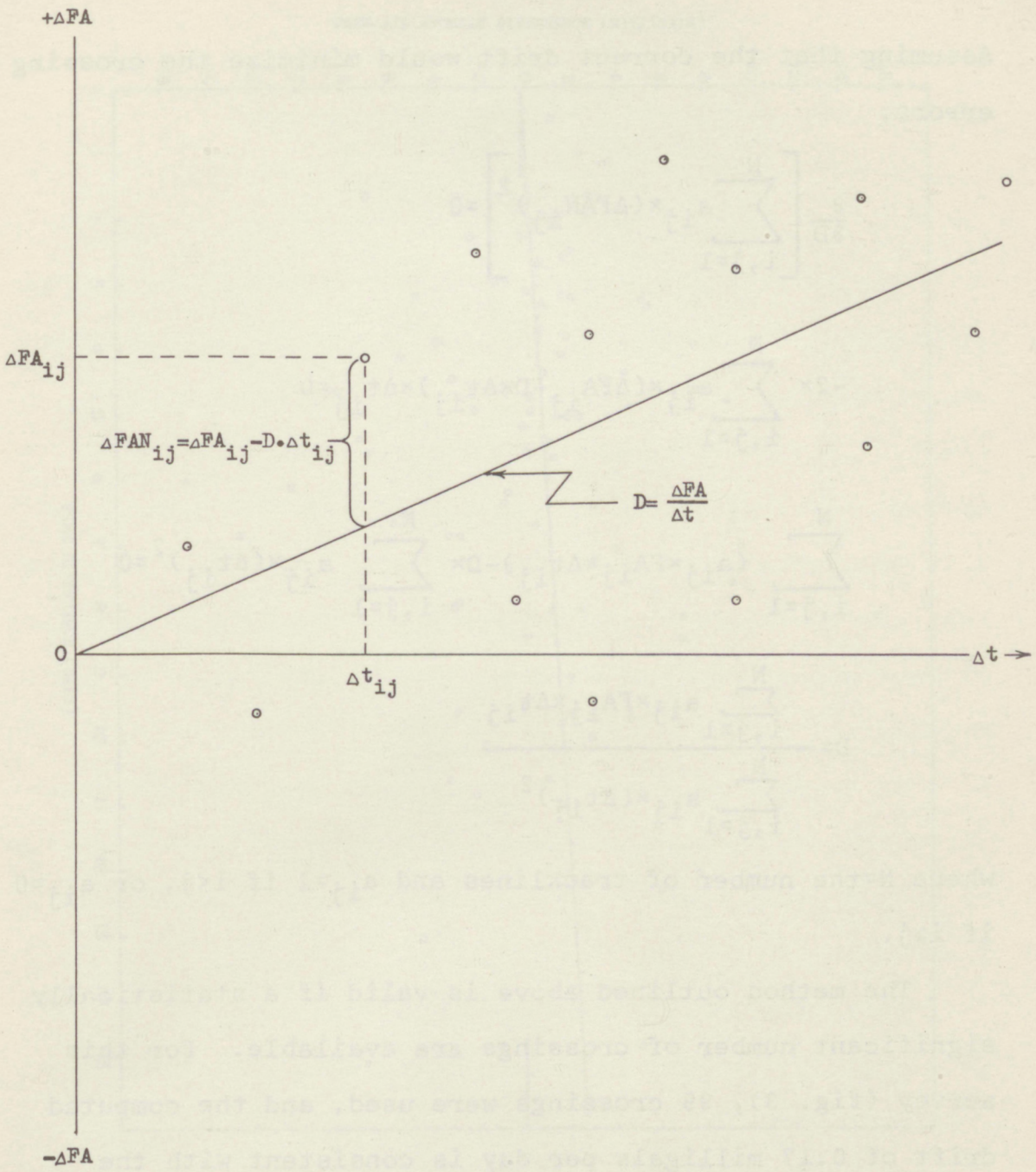

Figure 2. A statistical method for determining drift. The free-air anomaly difference for each crossing of the ship's track is plotted against the corresponding time difference. The drift, D, is the slope of the straight line through the origin which (in a least squares sense) most closely fits all the points (ΔFA_{ij},Δt_{ij}).

Assuming that the correct drift would minimize the crossing errors,

$$\frac{\partial}{\partial D}\left[\sum_{i,j=1}^{N} a_{ij}\times(\Delta FAN_{ij})^2\right]=0$$

$$-2\times\sum_{i,j=1}^{N} a_{ij}\times(\Delta FA_{ij}-D\times\Delta t_{ij})\times\Delta t_{ij}=0$$

$$\sum_{i,j=1}^{N}(a_{ij}\times FA_{ij}\times\Delta t_{ij})-D\times\sum_{i,j=1}^{N} a_{ij}\times(\Delta t_{ij})^2=0$$

$$D=\frac{\sum_{i,j=1}^{N} a_{ij}\times FA_{ij}\times\Delta t_{ij}}{\sum_{i,j=1}^{N} a_{ij}\times(\Delta t_{ij})^2}$$

where N=the number of tracklines and $a_{ij}=1$ if $i<j$, or $a_{ij}=0$ if $i\geq j$.

The method outlined above is valid if a statistically significant number of crossings are available. For this survey (fig. 3), 99 crossings were used, and the computed drift of 0.17 milligals per day is consistent with the gravimeter's drift history.

In the final stages of data processing, time profiles of the free-air anomaly were plotted on an automatic X-Y plotter. Residual discontinuities at course and speed

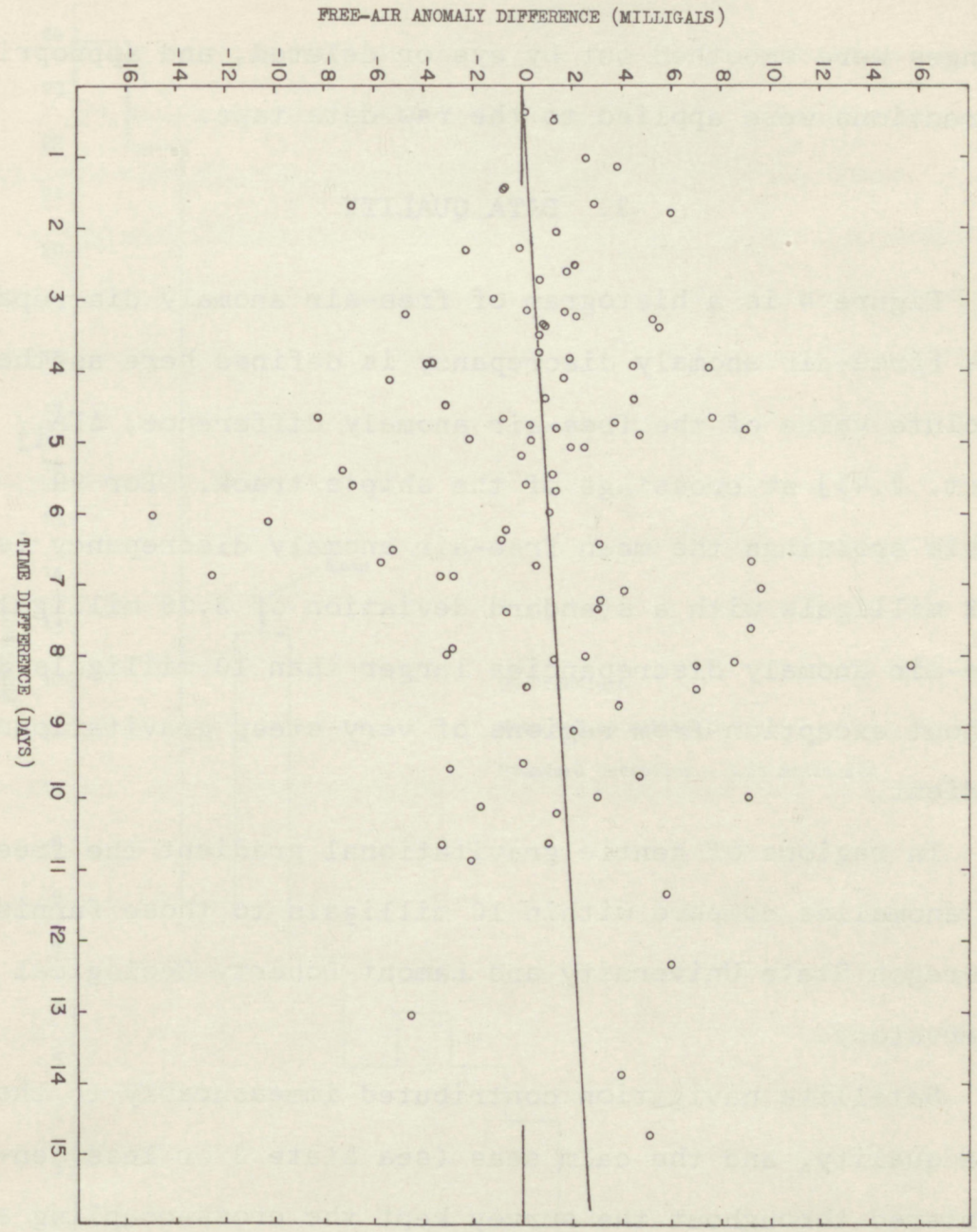

Figure 3. The free-air anomaly differences plotted against the corresponding time differences for 99 crossings of the ship's track. The slope of the solid line through the origin (0.17 milligals per day) is the drift of the gravimeter during this survey.

changes were smoothed out by eye or deleted, and appropriate corrections were applied to the raw data tape.

3. DATA QUALITY

Figure 4 is a histogram of free-air anomaly discrepancies [free-air anomaly discrepancy is defined here as the absolute value of the free-air anomaly difference, ΔFA_{ij} (sect. 2.4)] at crossings of the ship's track. For 99 usable crossings the mean free-air anomaly discrepancy is 3.48 milligals with a standard deviation of 3.28 milligals. Free-air anomaly discrepancies larger than 10 milligals are without exception from regions of very steep gravitational gradient.

In regions of gentle gravitational gradient the free-air anomalies compare within 10 milligals to those furnished by Oregon State University and Lamont-Doherty Geological Observatory.

Satellite navigation contributed immeasurably to the data quality, and the calm seas (sea state 3 or less) encountered throughout the survey kept the cross-coupling and off-leveling errors to a minimum.

4. DATA PRESENTATION

The data are presented in profile form with the free-air anomaly plotted above the corresponding bathymetry. All

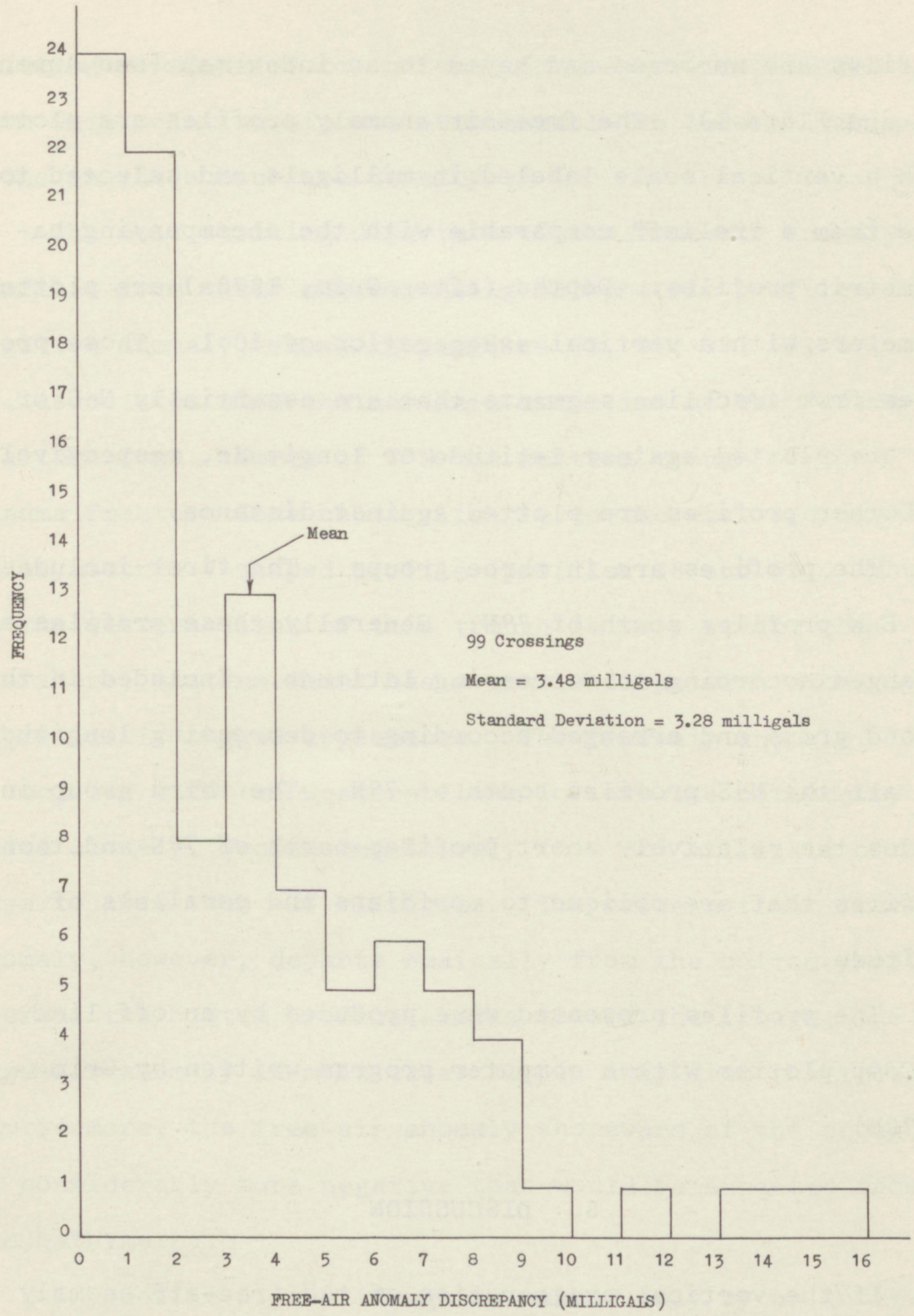

Figure 4. Histogram of free-air anomaly discrepancies at crossings of the ship's track.

profiles are numbered and keyed to an index map (see Appendix and Plate 1). The free-air anomaly profiles are plotted with a vertical scale labeled in milligals and selected to give them a "relief" comparable with the accompanying bathymetric profiles. Depths (after Grim, 1970a) are plotted in meters with a vertical exaggeration of 50:1. Those profiles from trackline segments that are essentially N-S or E-W are plotted against latitude or longitude, respectively. All other profiles are plotted against distance.

The profiles are in three groups. The first includes all E-W profiles south of 7°N. Generally these profiles are arranged according to decreasing latitude. Included in the second group and arranged according to decreasing longitude are all the N-S profiles south of 7°N. The third group includes the relatively short profiles north of 7°N and those profiles that are oblique to meridians and parallels of latitude.

The profiles presented were produced by an off line CalComp plotter with a computer program written by Grim (1970b).

5. DISCUSSION

If the vertical exaggeration of the free-air anomaly profiles is selected to give them about the same "relief" as the bathymetric profiles, then they should look like

filtered versions of the bottom topography. Departures from this relationship are attributable to lateral variations in the subsurface density.

The most striking departure of the free-air anomaly profiles from their corresponding bathymetric profiles is a negative anomaly, shown in profiles 33, 36, 38, 53, 54, and 55, associated with the northern extension of the Panama Fracture Zone. North of 7°N the western trough of the Panama Fracture Zone bends slightly to the west and develops an asymmetric V-shaped profile (profiles 38 and 55). Whereas the western flank of this trough is very steep, the nearshore, eastern flank has a gentle slope with a characteristically rugged appearance. The free-air anomaly associated with the western flank follows the bathymetry quite closely, decreasing sharply from +25 milligals or more to less than -25 milligals. The eastern flank free-air anomaly, however, departs radically from the bottom profile; whereas the bottom profile slopes toward the trough, the free-air anomaly in most cases slopes away from the trough. Furthermore, the free-air anomaly shoreward of the trough is considerably more negative than would be expected from the bathymetry.

In profile 55 the trough is marked only by an inflexion in the free-air anomaly. A -68-milligal low in the free-air anomaly profile lies about 40 km shoreward of the trough.

Similarly, the -62-milligal low of profile 36 is displaced about 20 km east of the trough. The free-air anomaly of profile 38, on the other hand, apparently does not continue to decrease east of the trough. Profiles 33, 53, and the extreme eastern end of profile 54 show an inverse relationship between the slopes of the free-air anomaly and the characteristically rugged bathymetry.

These observations are consistent with the occurrence of a deep, sediment-filled depression that van Andel et al. (1971) have proposed to exist between the Cocos and Coiba Ridges.

Another similar departure of the free-air anomaly from the bathymetry is the negative anomaly associated with a gentle bathymetric depression extending from the eastern edge of the survey area (80°W) to about 81°40'W on the eastern flank of the Coiba Ridge. Although the axis of this depression is not crossed by any of the survey lines, it appears to be nearly coincident with profile 31. The free-air anomaly, on the other hand, continues to decrease at least as far north as profile 1.

It is evident that this free-air anomaly pattern is a continuation of the negative anomaly belt (Hayes, 1966) that extends around the Gulf of Panama from the Peru-Chile Trench. Hayes suggested that the most significant contribution to this negative anomaly belt may be the "edge effect" (Worzel,

1965) of a steep continental slope. However, the observation that west of 80°W the axis of this negative anomaly belt lies well shoreward of the bathymetric depression axis is better explained by the sequence of deep, sediment-filled marginal troughs proposed by van Andel et al. (1971).

Especially evident in profile 3 is the departure of the free-air anomaly from the bathymetry on the eastern flanks of the Cocos and Coiba Ridges. West of the Panama Fracture Zone the eastern flank of the Cocos Ridge rises rather uniformly while the free-air anomaly levels off west of 83°40'W. The free-air anomaly centered over the crest of the Coiba Ridge falls off more rapidly to the east than might be expected from the bathymetry. These deviations of the free-air anomaly from the bottom topography are the reflection of thick accumulations of sediment on the eastern flanks of both ridges (van Andel et al., 1971, figs. 5B and 11G). This profile also suggests that there is no large-scale change in crustal structure across the Panama Fracture Zone.

The entire survey area may be slightly out of isostatic adjustment, as indicated by an average free-air anomaly of between +10 and +20 milligals.

6. ACKNOWLEDGEMENTS

I thank the officers and crew of the National Oceanic and Atmospheric Administration Ship OCEANOGRAPHER who made this study possible. Paul Grim furnished the data presented in this report. He also supplied most of the computer programs used and assisted in many ways throughout this study. Additional gravity data were provided by Dr. Richard Couch, Oregon State University, and Manik Talwani, Lamont-Doherty Geological Observatory. R. K. Lattimore, Paul Grim, and Dr. George Peter assisted by reviewing the manuscript.

7. REFERENCES

Graf, A. and R. Schulze (1961), Improvements in the sea gravimeter Gss2, J. Geophys. Res. 66, 1811-1821.

Grim, P. J. (1970a), Bathymetric and magnetic anomaly profiles from a survey south of Panama and Costa Rica, (unpublished report) ESSA Tech. Memo, ERLTM-AOML 9. (Environmental Research Laboratories, Boulder, Colorado 80302).

Grim, P. J. (1970b), Computer program for automatic plotting of bathymetric and magnetic anomaly profiles, (unpublished report) ESSA Tech. Memo, ERLTM-AOML 8. (Environmental Research Laboratories, Boulder, Colorado 80302).

Guier, W. H. (1966), Satellite navigation using integral Doppler data -- the AN/SRN-9 equipment, J. Geophys. Res. 71, 5903-5910.

Hayes, D. E. (1966), A geophysical investigation of the Peru-Chile trench, Marine Geology 4, 309-351.

Orlin, H. and D. V. Sibila (1966), General instructions, gravity observations at sea, part II: askania stable platform mounted seagravimeter, U. S. Department of Commerce, ESSA, Coast and Geodetic Survey.

Schulze, R (1962), Automation of the sea gravimeter Gss2, J. Geophys. Res. 67, 3397-3401.

Stansell, P. A., Jr. (1970), The Navy navigation satellite system: description and status, The International Hydrographic Review, XLVII, 51-70.

van Andel, T. H., G. R. Heath, B. T. Malfait, D. F. Heinrichs, and J. I. Ewing (1971), Tectonics of the Panama Basin, eastern equatorial Pacific, Geol. Soc. Amer. Bull. 82, 1489-1508.

Woollard, G. P. and J. C. Rose (1963), International Gravity Measurements, Society of Exploration Geophysicists, Tulsa, Oklahoma, 518 p.

Worzel, J. L. (1965), Deep structure of continental margins and mid-ocean ridges, In: W. F. Whittard and R. Bradshaw (Editors), Submarine Geology and Geophysics -- Colston Papers, Butterworth, Washington, D.C., 335-359.

APPENDIX

Profiles

The following pages display the computer-produced profiles from the survey area

Profile	Page	Profile	Page	Profile	Page	Profile	Page
1	22	14	35	27	23	42	27
3	24	15	49	28	44	43	37
4	40	16	36	29	51	44	29
5	26	17	25	30	44	45	43
6	37	18	39	31	23	46	31
7	28	19	49	32	48	47	38
8	42	20	40	33	48	48	29
9	30	21	27	34	46	49	38
10	34	22	41	36	46	50	31
11	32	23	49	38	47	51	34
12	51	24	42	39	37	52	50
13A	33	25	51	40	25	53	48
13B	33	26	43	41	43	54	47
						55	45
						62	45

Table 1. Index of Profiles

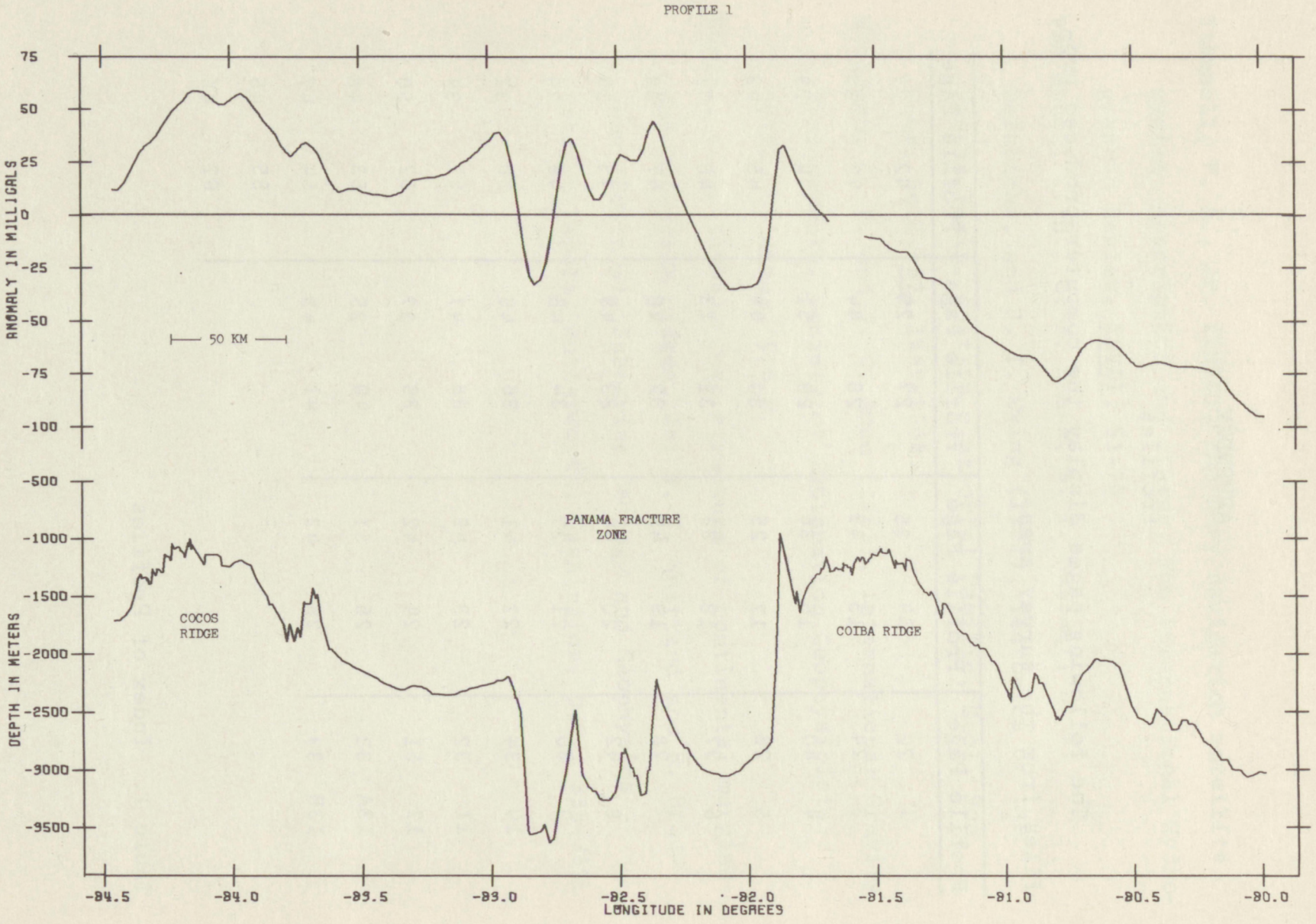
PROFILE 1
75
50
25
0
-25
-50
-75
-100
ANOMALY IN MILLIGALS
50 KM
-500
-1000
-1500
-2000
-2500
-3000
-3500
DEPTH IN METERS
PANAMA FRACTURE ZONE
COCOS RIDGE
COIBA RIDGE
-84.5
-84.0
-83.5
-83.0
-82.5
-82.0
-81.5
-81.0
-80.5
-80.0
LONGITUDE IN DEGREES

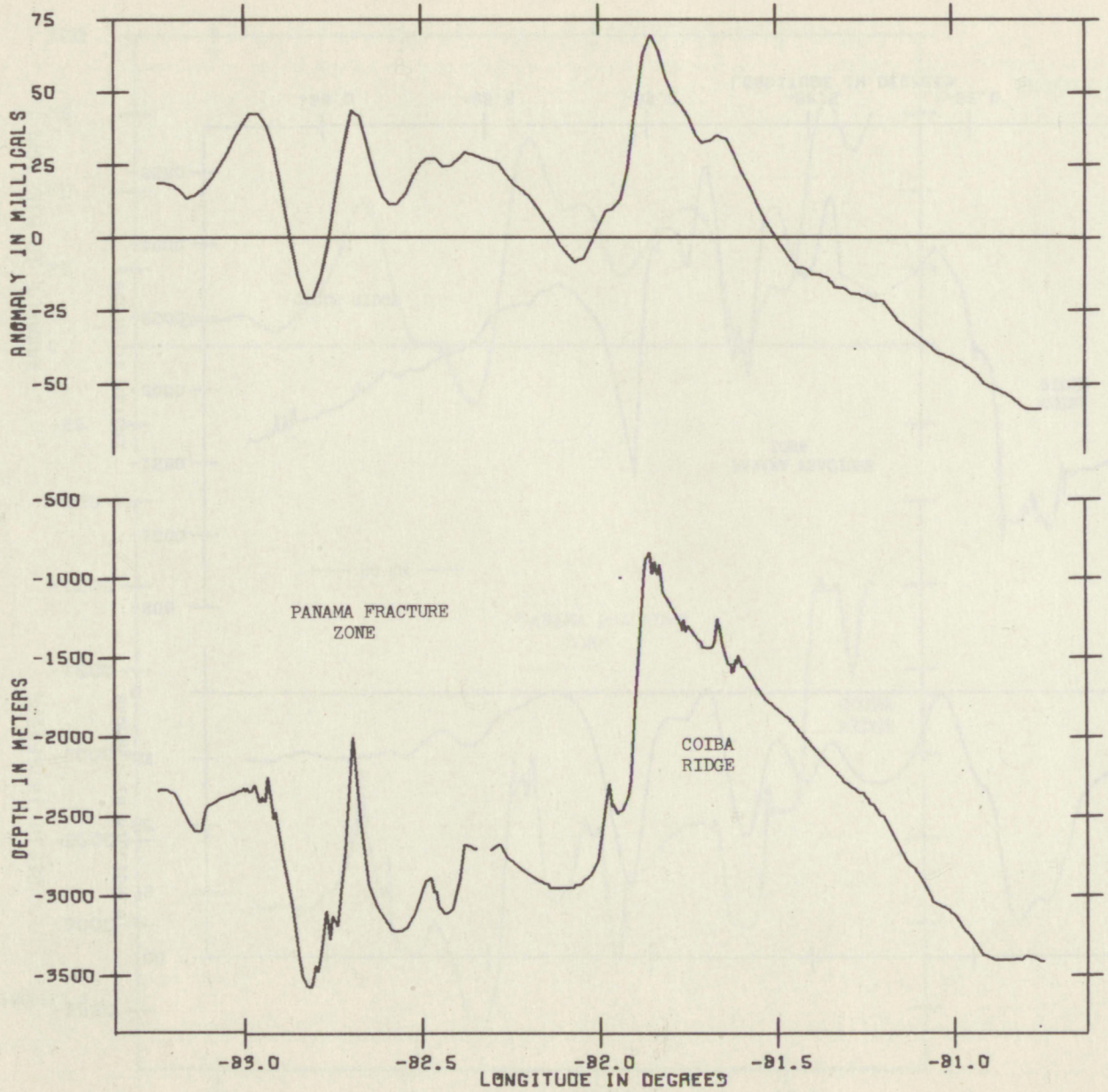

PROFILE 31

50 KM

PROFILE 27

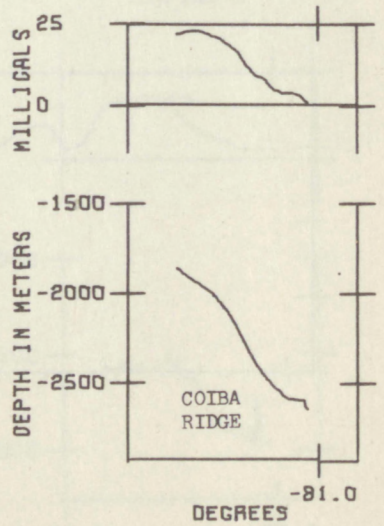

PROFILE 3

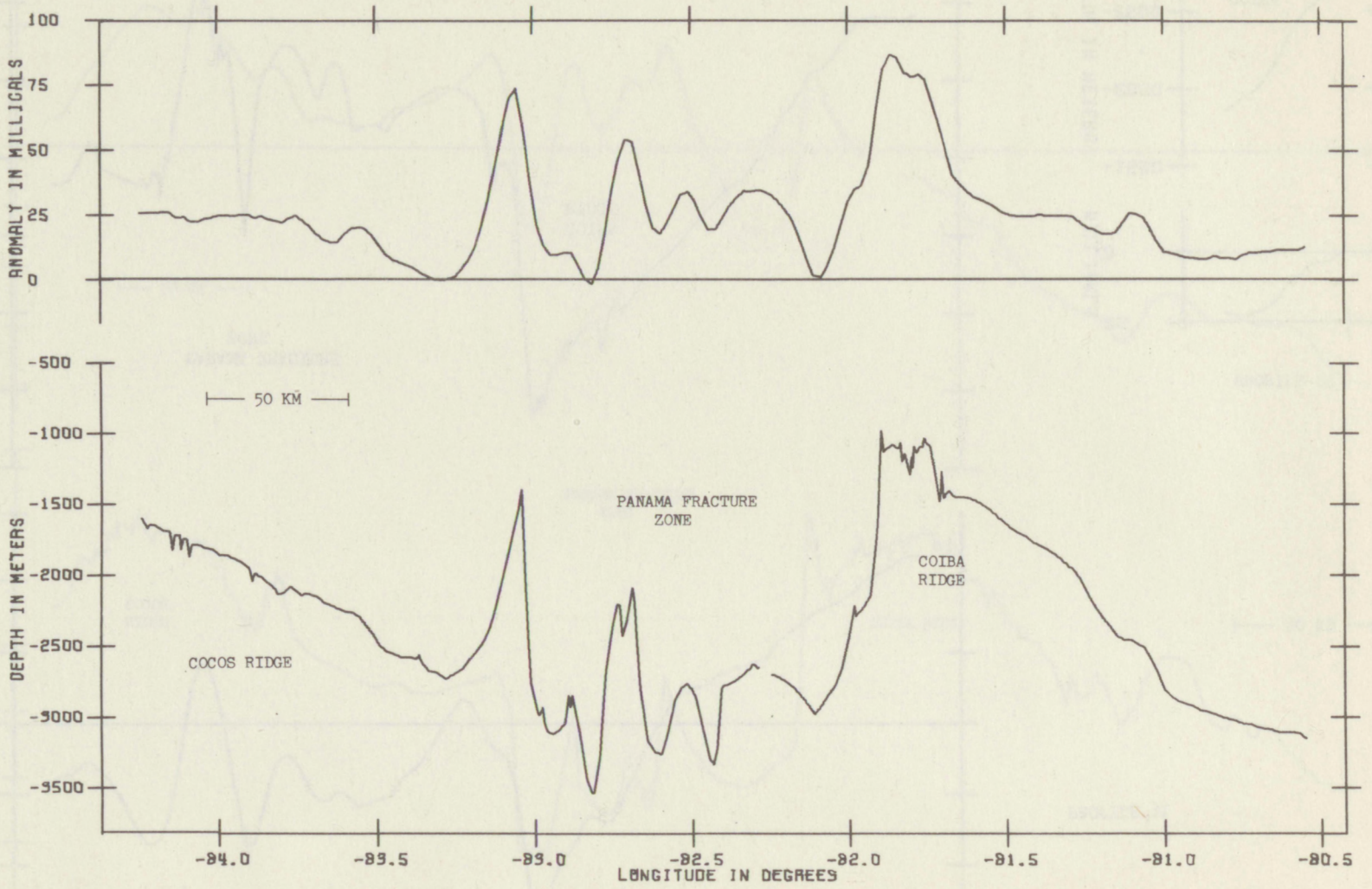
100
75
50
25
0
ANOMALY IN MILLIGALS
-500
-1000
-1500
-2000
-2500
-3000
-3500
DEPTH IN METERS
50 KM
PANAMA FRACTURE
ZONE
COCOS RIDGE
COIBA
RIDGE
-84.0
-83.5
-83.0
-82.5
-82.0
-81.5
-81.0
-80.5
LONGITUDE IN DEGREES

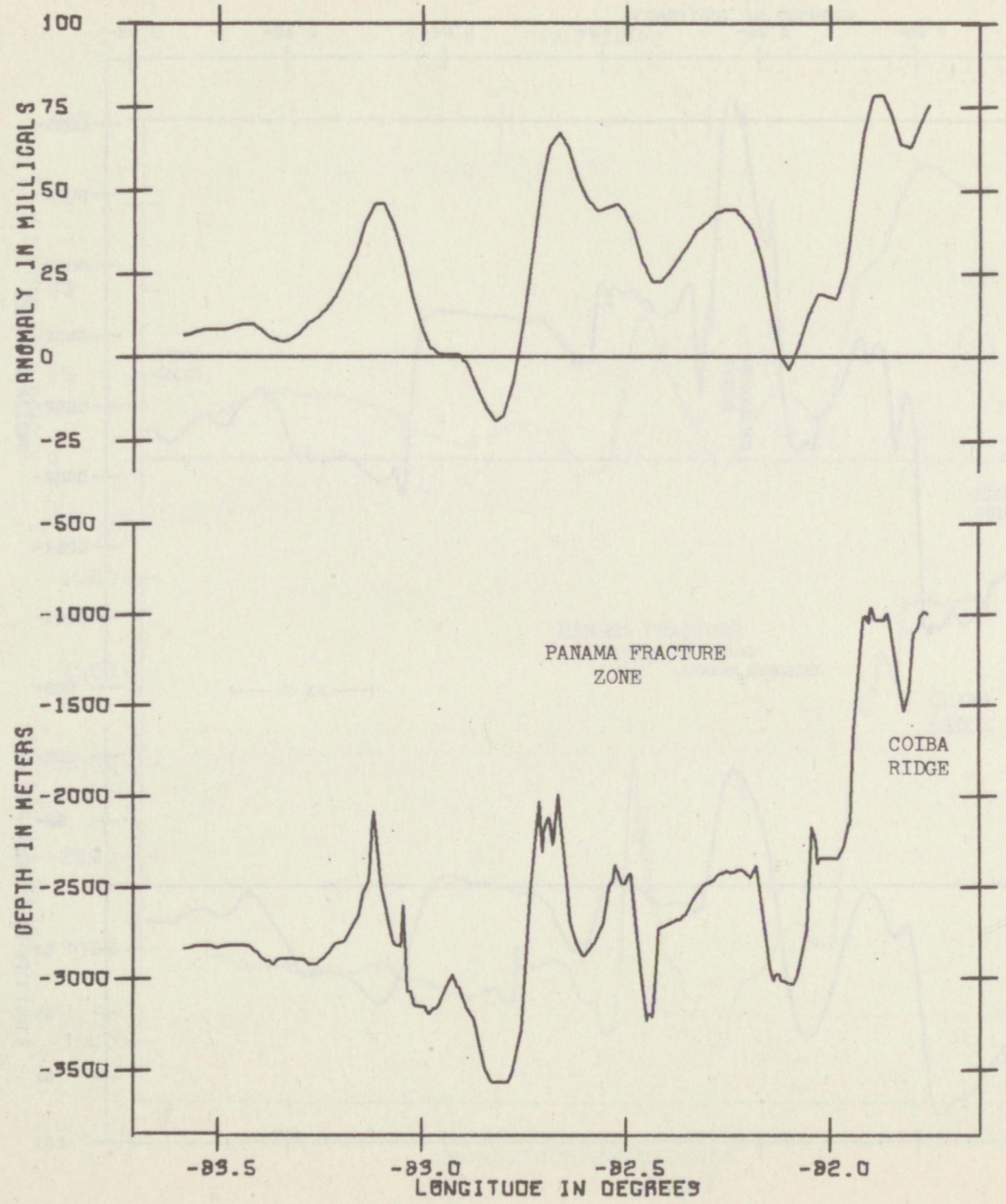

PROFILE 40

50 KM

PROFILE 17

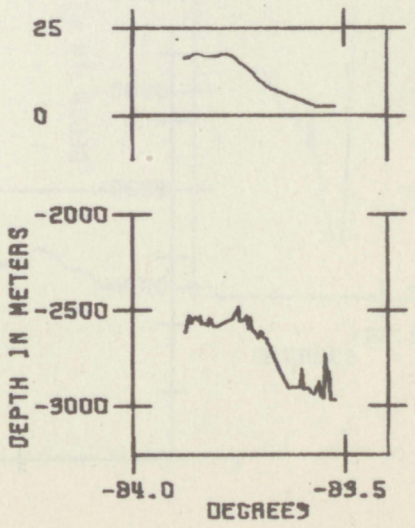

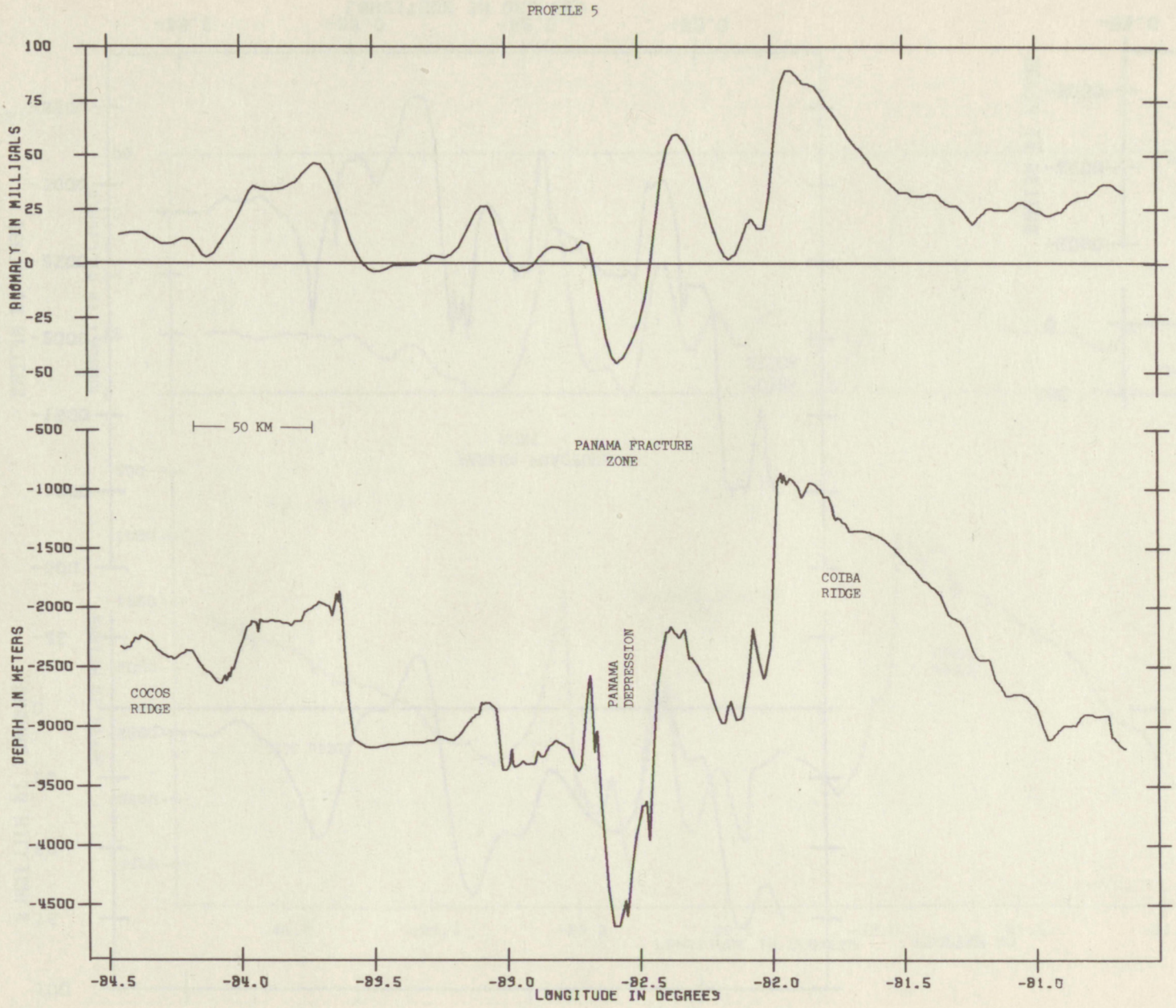
PROFILE 5
ANOMALY IN MILLIGALS
100
75
50
25
0
-25
-50
50 KM
PANAMA FRACTURE ZONE
DEPTH IN METERS
-500
-1000
-1500
-2000
-2500
-3000
-3500
-4000
-4500
COCOS RIDGE
PANAMA DEPRESSION
COIBA RIDGE
-84.5
-84.0
-83.5
-83.0
-82.5
-82.0
-81.5
-81.0
LONGITUDE IN DEGREES

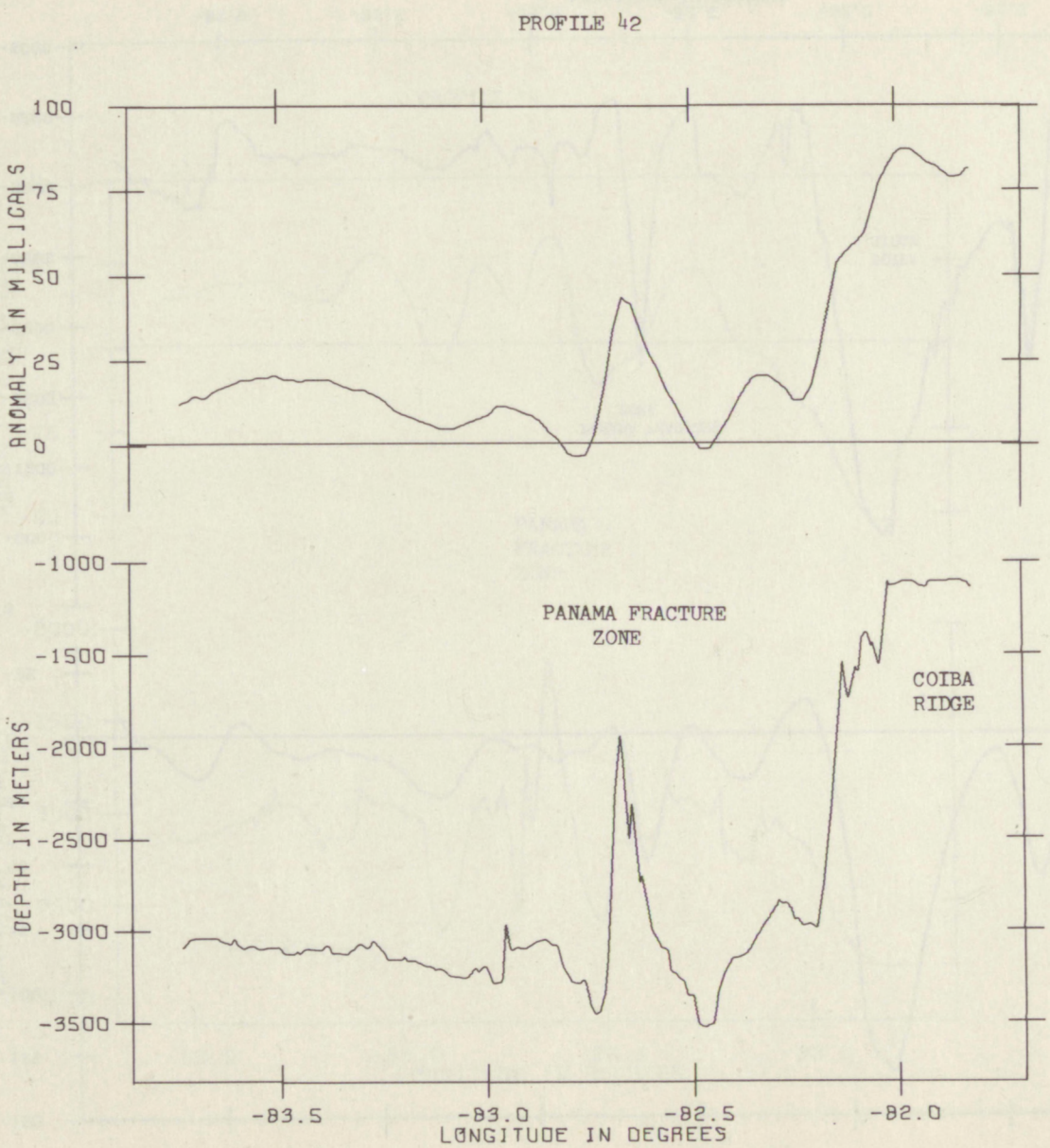
PROFILE 42
100
75
50
25
0
ANOMALY IN MILLIGALS
-1000
-1500
-2000
-2500
-3000
-3500
DEPTH IN METERS
PANAMA FRACTURE ZONE
COIBA RIDGE
-83.5
-83.0
-82.5
-82.0
LONGITUDE IN DEGREES

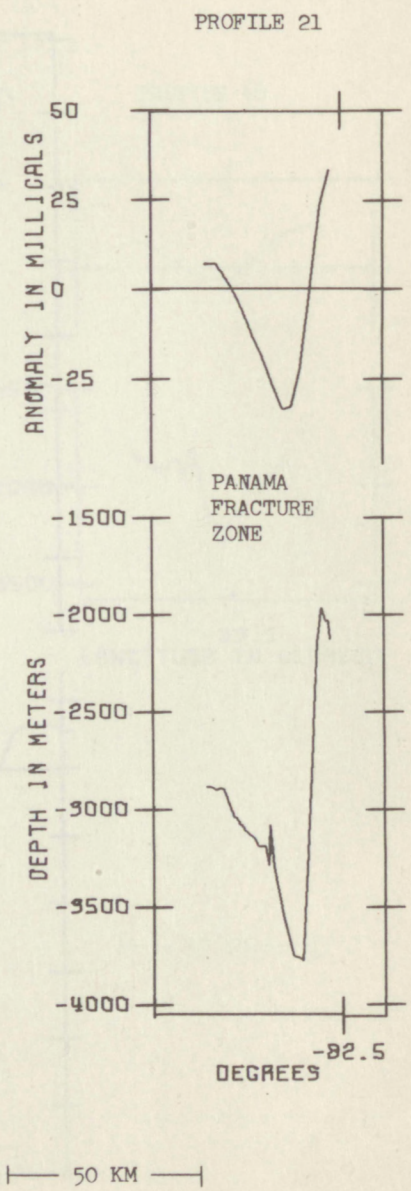
PROFILE 21
50
25
0
-25
ANOMALY IN MILLIGALS
PANAMA FRACTURE ZONE
-1500
-2000
-2500
-3000
-3500
-4000
DEPTH IN METERS
-82.5
DEGREES
50 KM

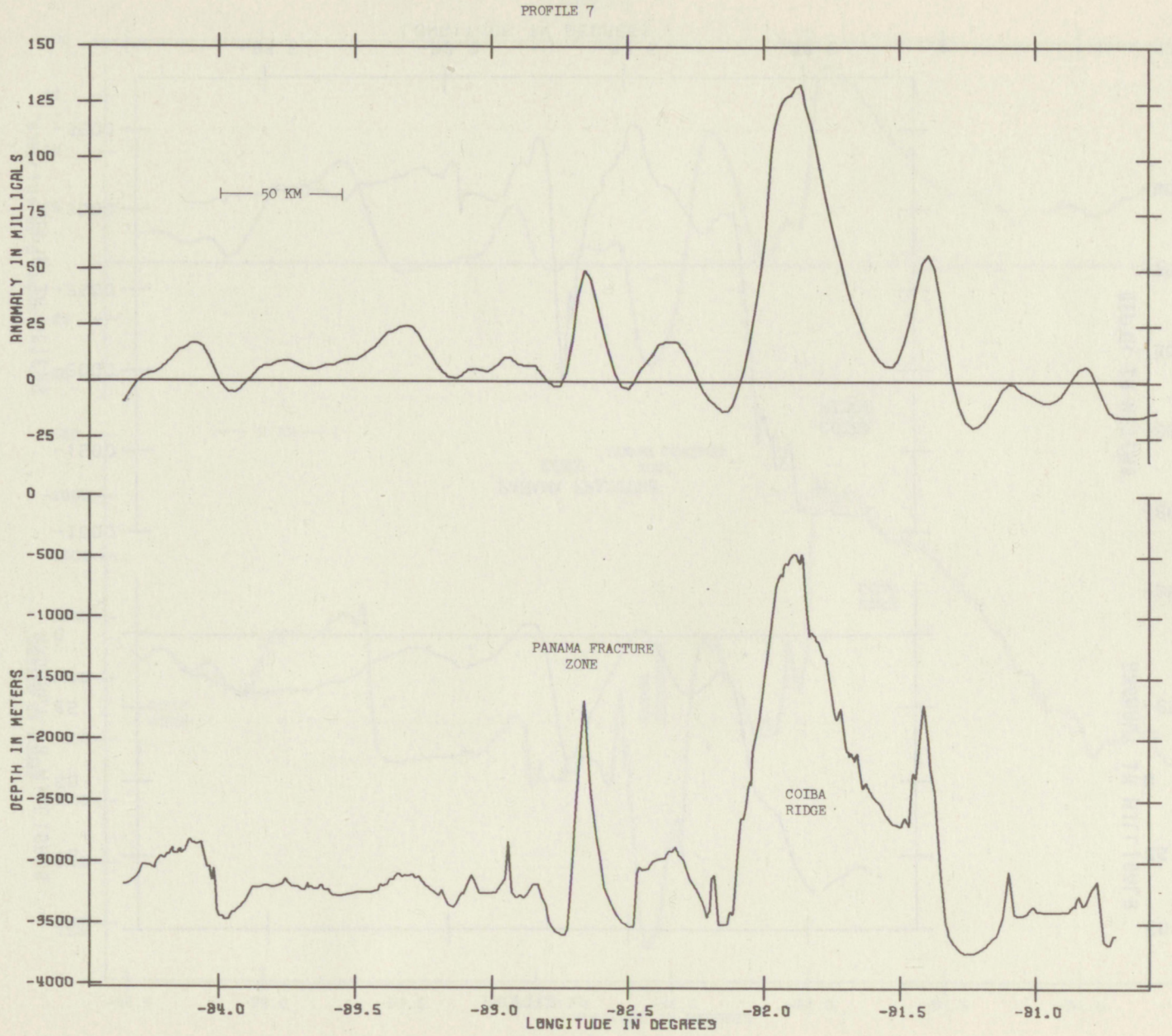
PROFILE 7
150
125
100
75
50
25
0
-25
ANOMALY IN MILLIGALS
50 KM
0
-500
-1000
-1500
-2000
-2500
-3000
-3500
-4000
DEPTH IN METERS
PANAMA FRACTURE ZONE
COIBA RIDGE
-84.0
-83.5
-83.0
-82.5
-82.0
-81.5
-81.0
LONGITUDE IN DEGREES

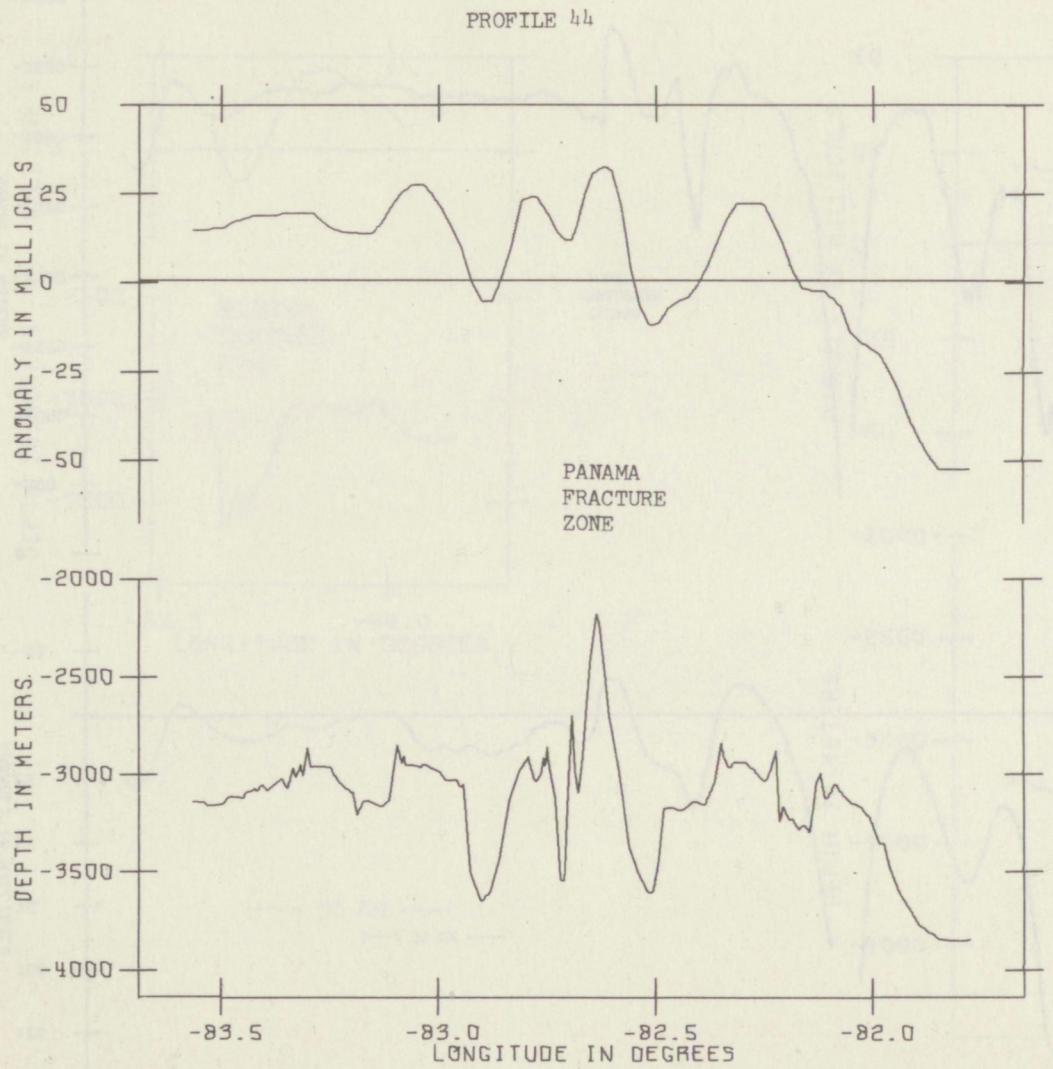
PROFILE 44
50
25
0
-25
-50
ANOMALY IN MILLIGALS
PANAMA
FRACTURE
ZONE
-2000
-2500
-3000
-3500
-4000
DEPTH IN METERS
-83.5
-83.0
-82.5
-82.0
LONGITUDE IN DEGREES

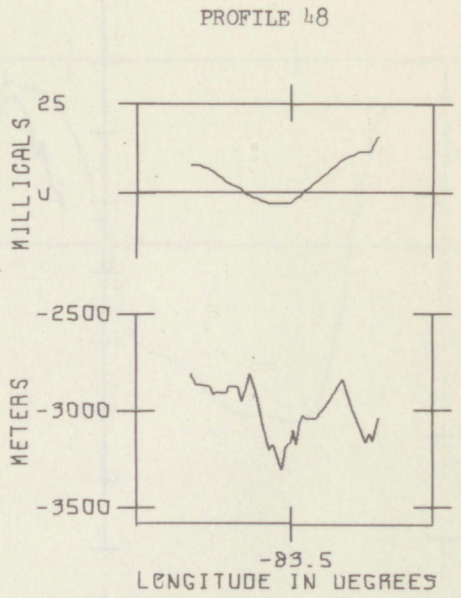
PROFILE 48
25
MILLIGALS
-2500
-3000
-3500
METERS
-83.5
LONGITUDE IN DEGREES

50 KM

PROFILE 9

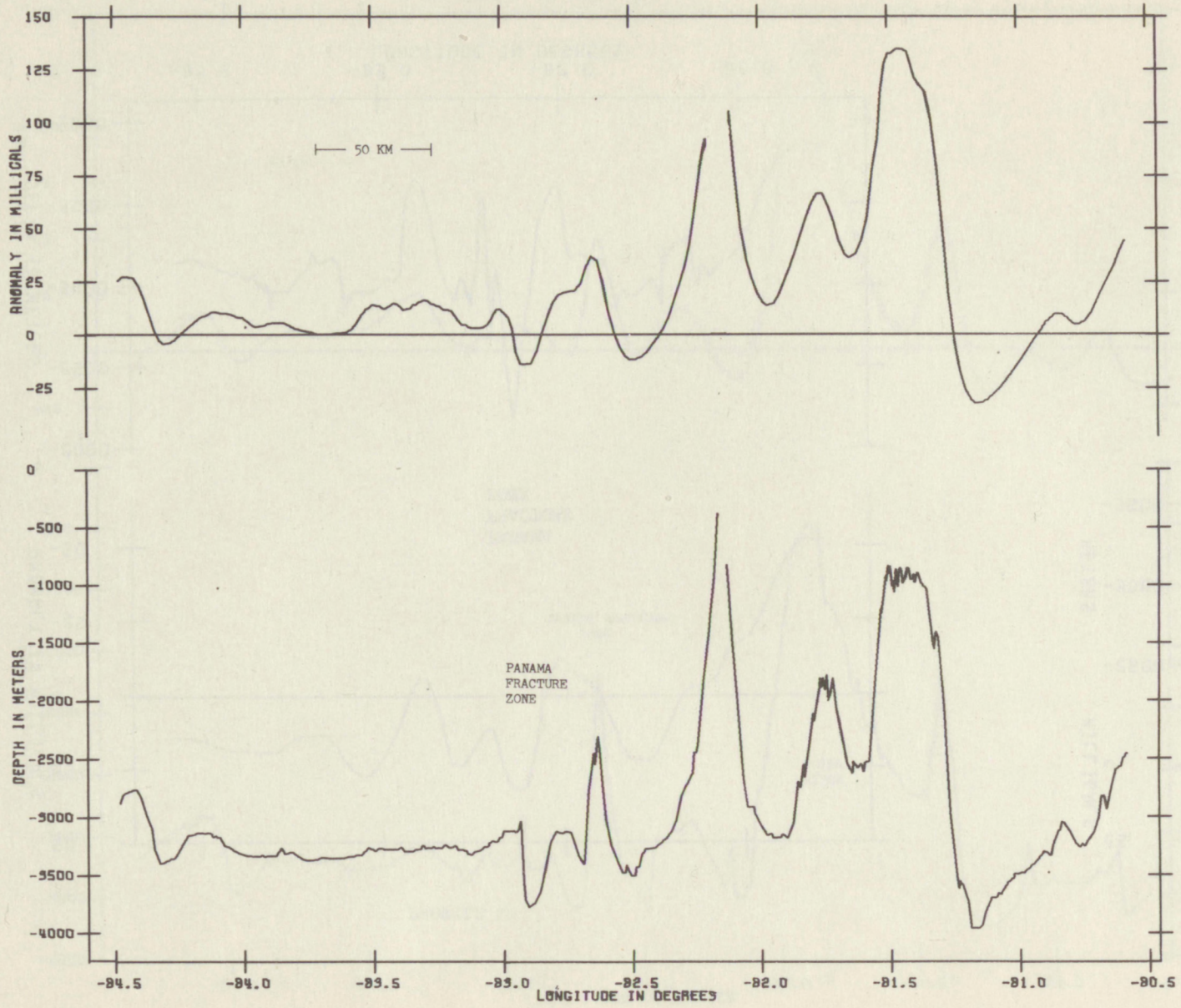
150
125
100
75
50
25
0
-25
ANOMALY IN MILLIGALS
50 KM
0
-500
-1000
-1500
-2000
-2500
-3000
-3500
-4000
DEPTH IN METERS
PANAMA
FRACTURE
ZONE
-84.5
-84.0
-83.5
-83.0
-82.5
-82.0
-81.5
-81.0
-80.5
LONGITUDE IN DEGREES

PROFILE 50

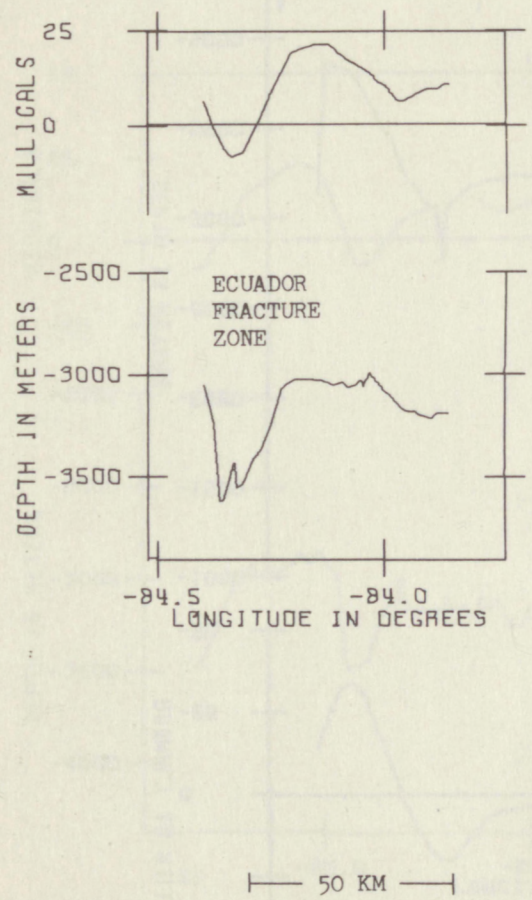

50 KM

PROFILE 46

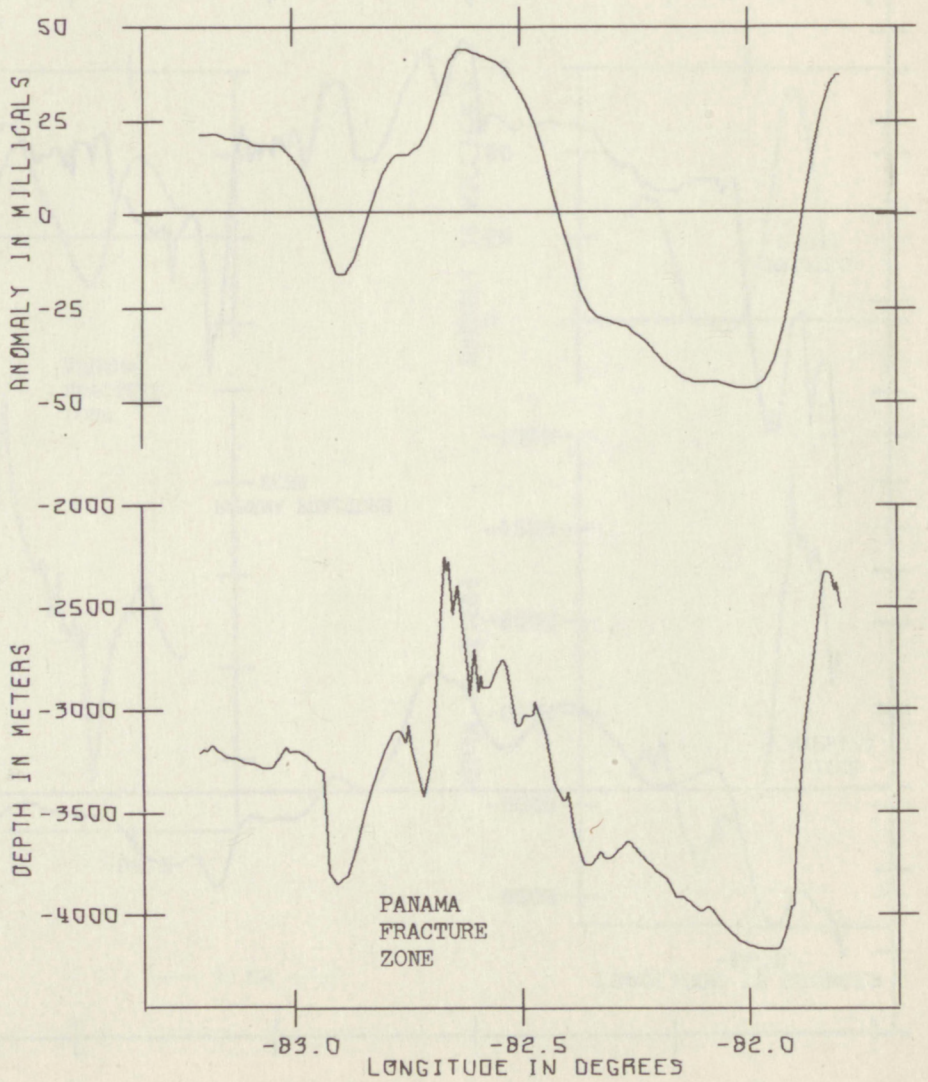

PROFILE 11

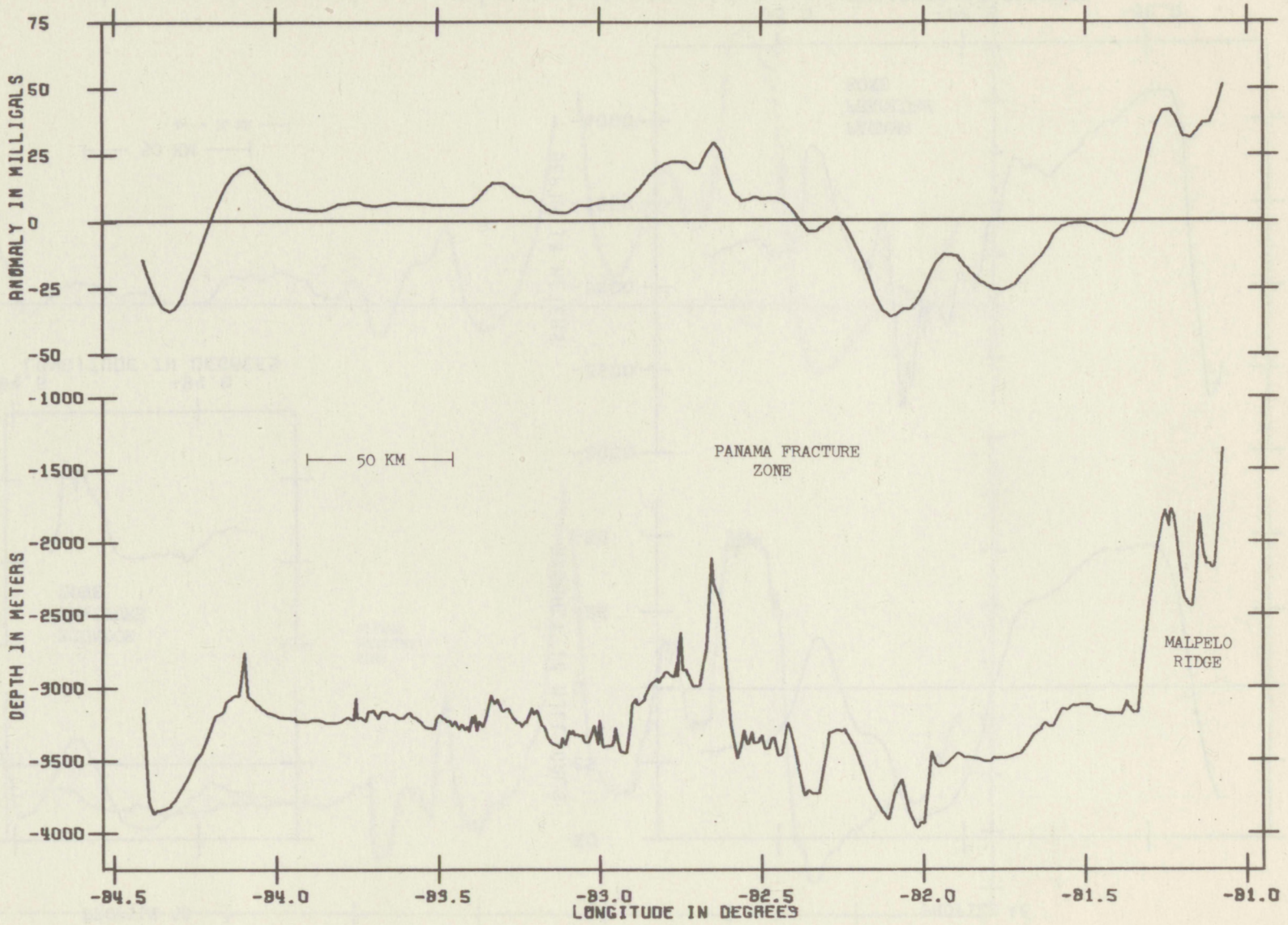
75
50
25
0
-25
-50
ANOMALY IN MILLIGALS
-1000
-1500
-2000
-2500
-3000
-3500
-4000
DEPTH IN METERS
50 KM
PANAMA FRACTURE ZONE
MALPELO RIDGE
-84.5
-84.0
-83.5
-83.0
-82.5
-82.0
-81.5
-81.0
LONGITUDE IN DEGREES

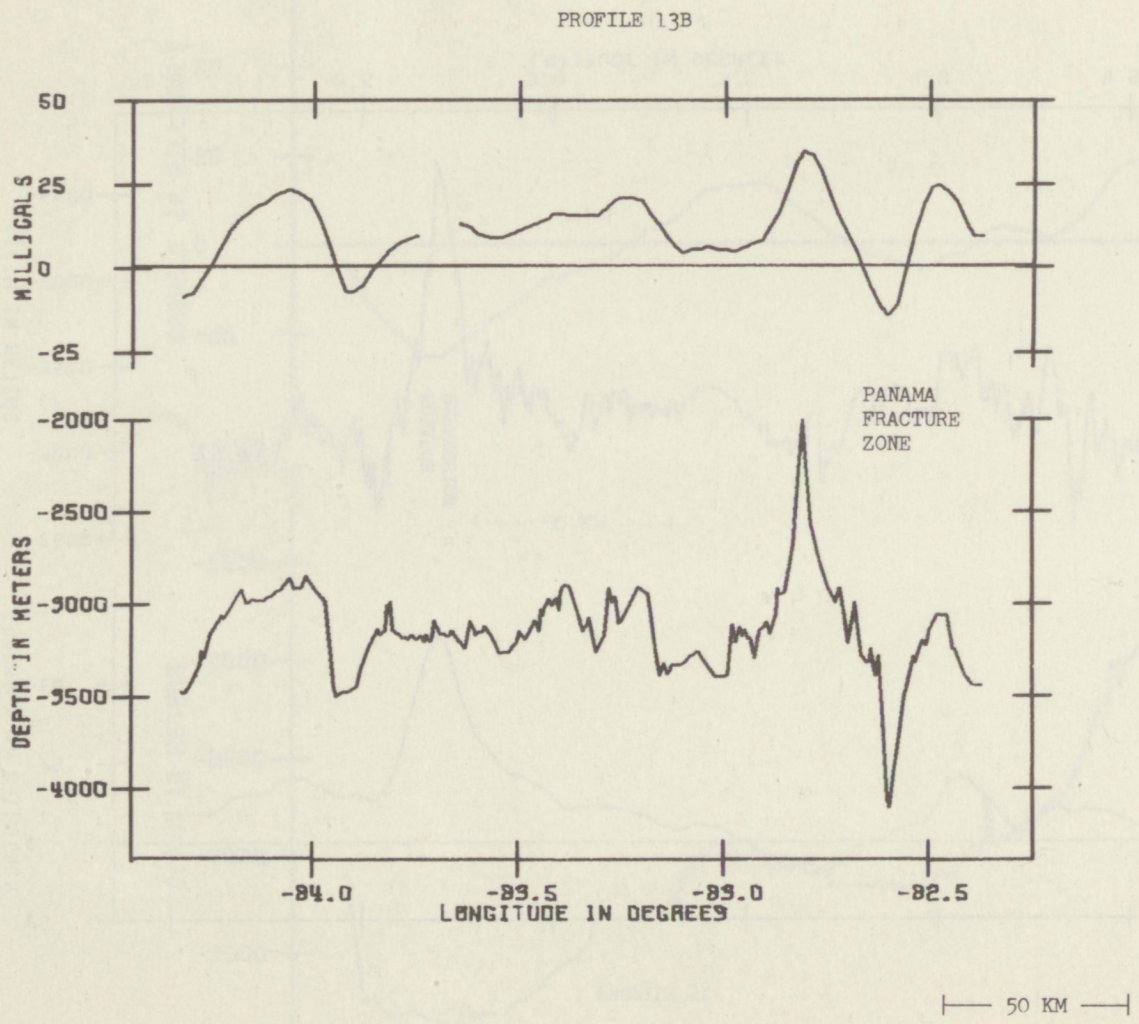
PROFILE 13B
50
25
0
-25
MILLIGALS
-2000
-2500
-3000
-3500
-4000
DEPTH IN METERS
PANAMA
FRACTURE
ZONE
-84.0
-83.5
-83.0
-82.5
LONGITUDE IN DEGREES
50 KM

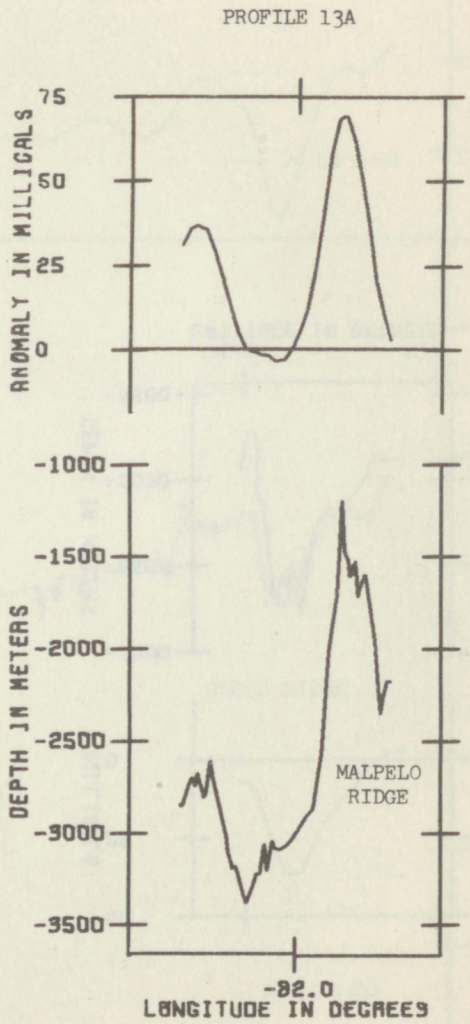
PROFILE 13A
75
50
25
0
ANOMALY IN MILLIGALS
-1000
-1500
-2000
-2500
-3000
-3500
DEPTH IN METERS
MALPELO
RIDGE
-82.0
LONGITUDE IN DEGREES

PROFILE 51

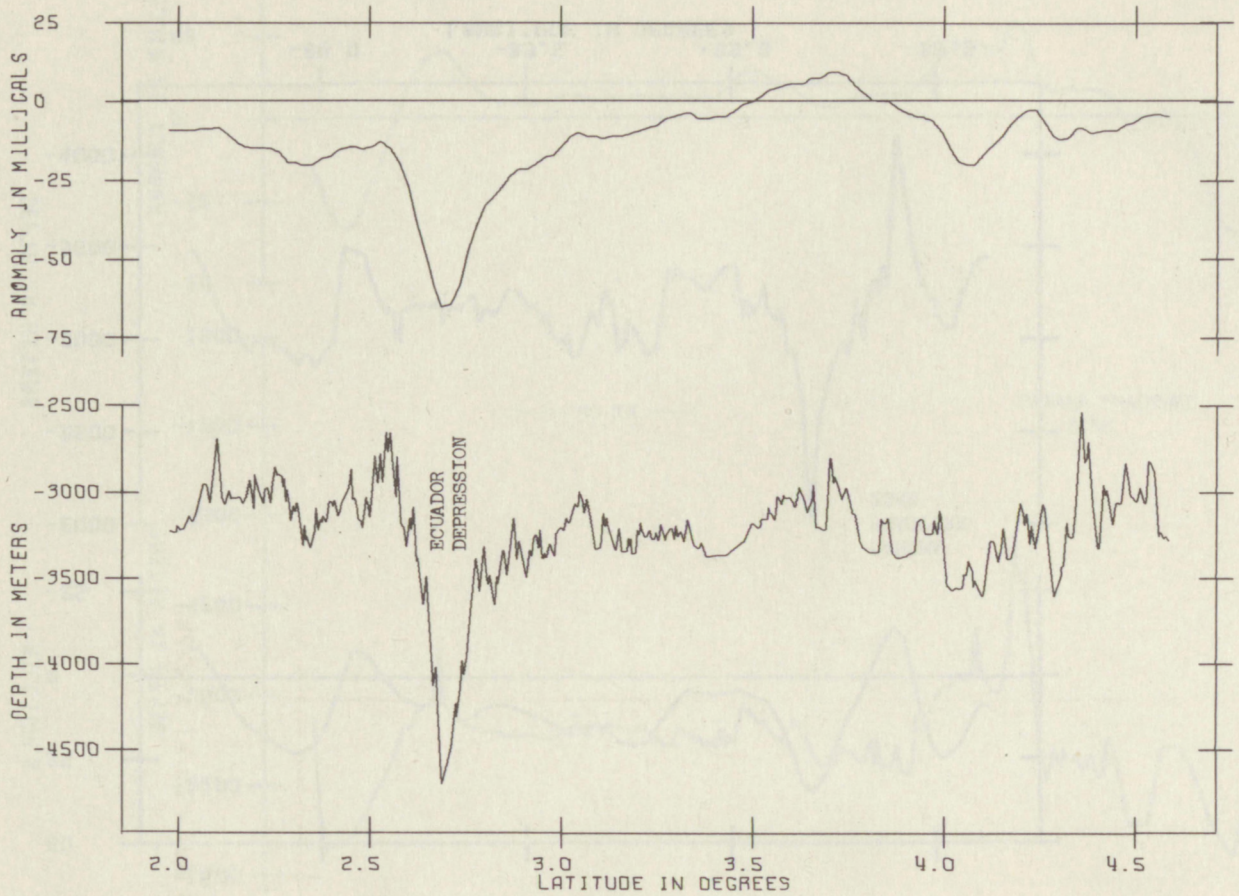

PROFILE 10

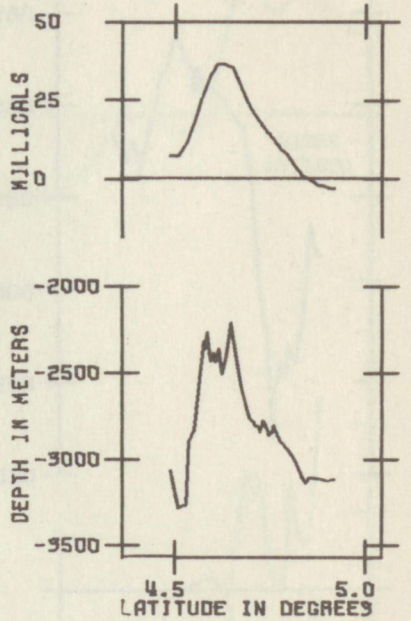

50 KM

PROFILE 14

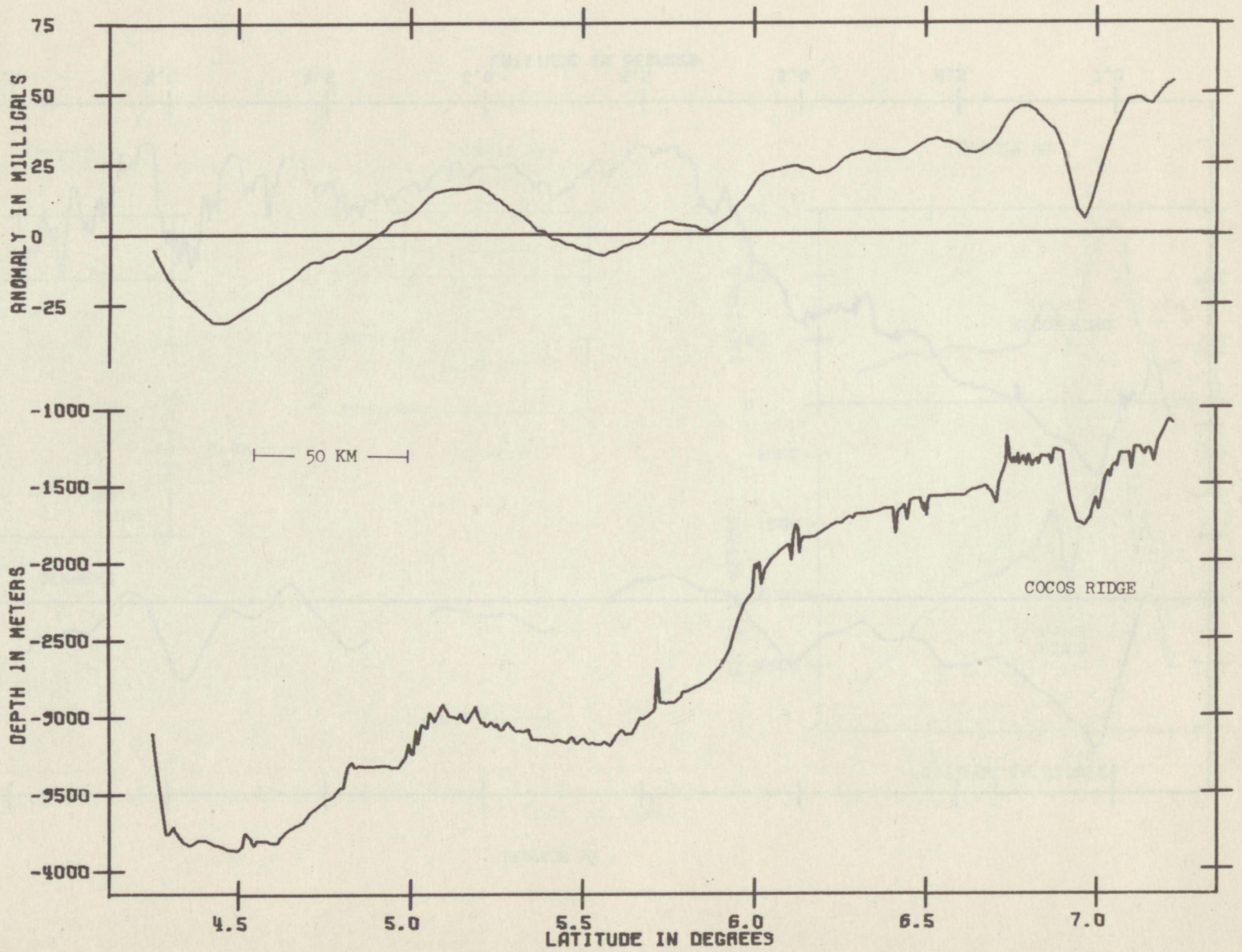
75
50
25
0
-25
ANOMALY IN MILLIGALS
-1000
-1500
-2000
-2500
-3000
-3500
-4000
DEPTH IN METERS
50 KM
COCOS RIDGE
4.5
5.0
5.5
6.0
6.5
7.0
LATITUDE IN DEGREES

PROFILE 16

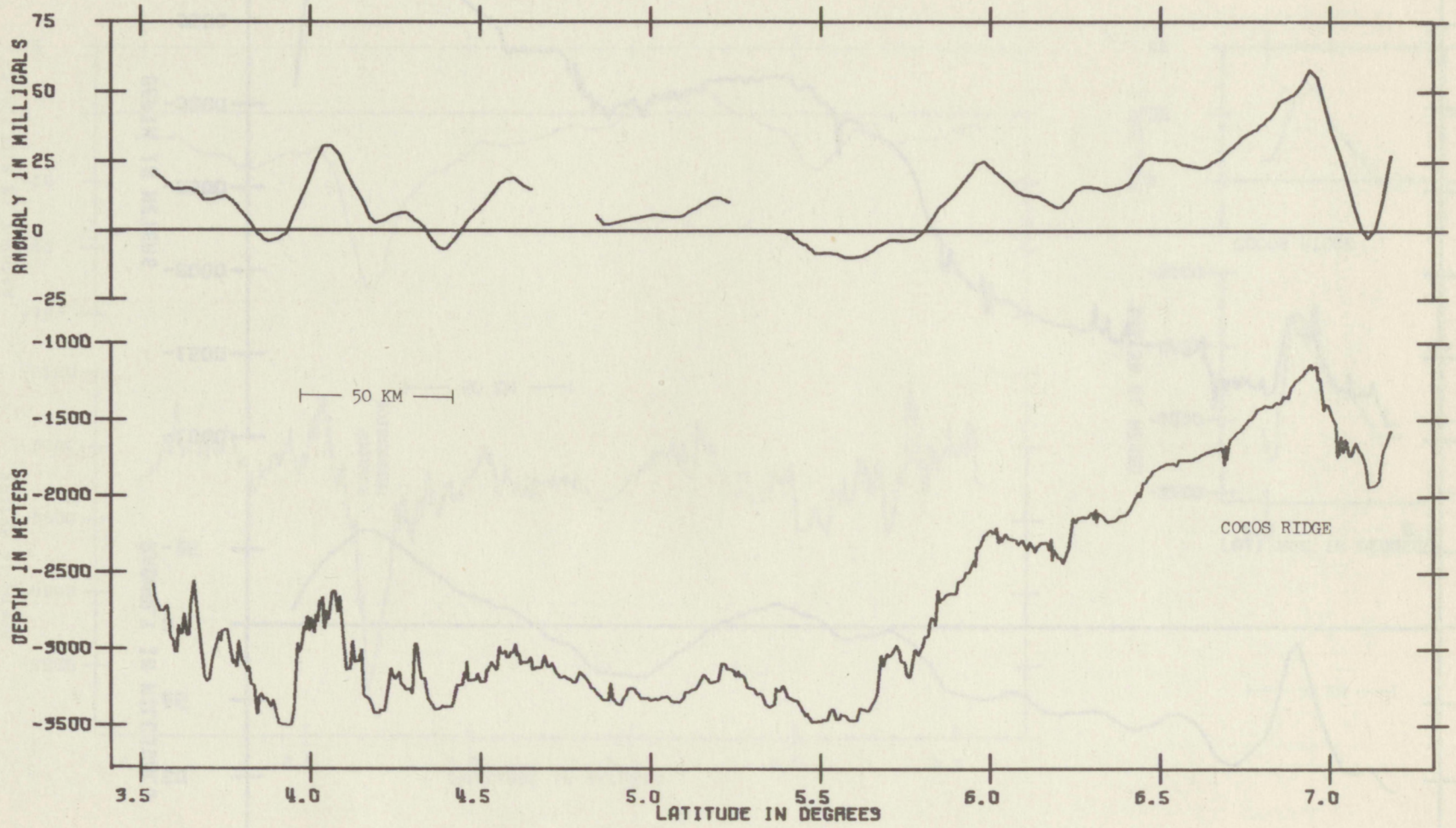
ANOMALY IN MILLIGALS
75
50
25
0
-25
DEPTH IN METERS
-1000
-1500
-2000
-2500
-3000
-3500
50 KM
COCOS RIDGE
3.5
4.0
4.5
5.0
5.5
6.0
6.5
7.0
LATITUDE IN DEGREES

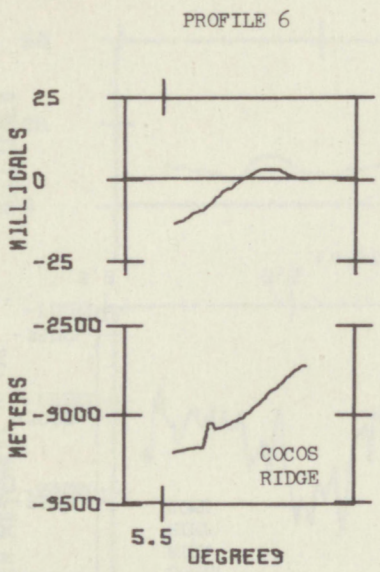
PROFILE 6
25
0
-25
MILLIGALS
-2500
-9000
-9500
METERS
COCOS
RIDGE
5.5
DEGREES

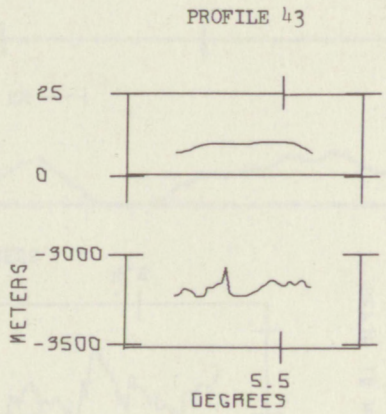
PROFILE 43
25
0
-3000
-3500
METERS
5.5
DEGREES

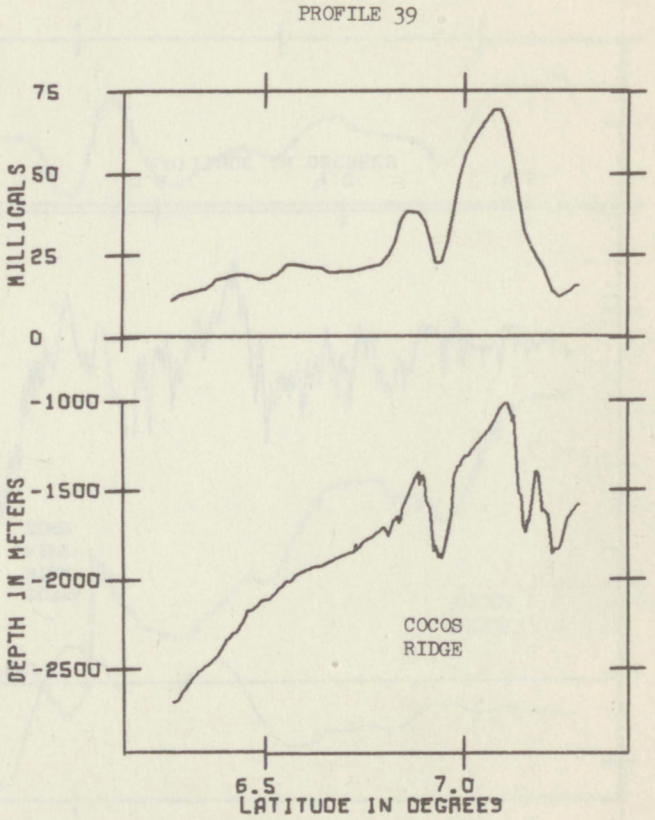
PROFILE 39
75
50
25
0
MILLIGALS
-1000
-1500
-2000
-2500
DEPTH IN METERS
COCOS
RIDGE
6.5
7.0
LATITUDE IN DEGREES

50 KM

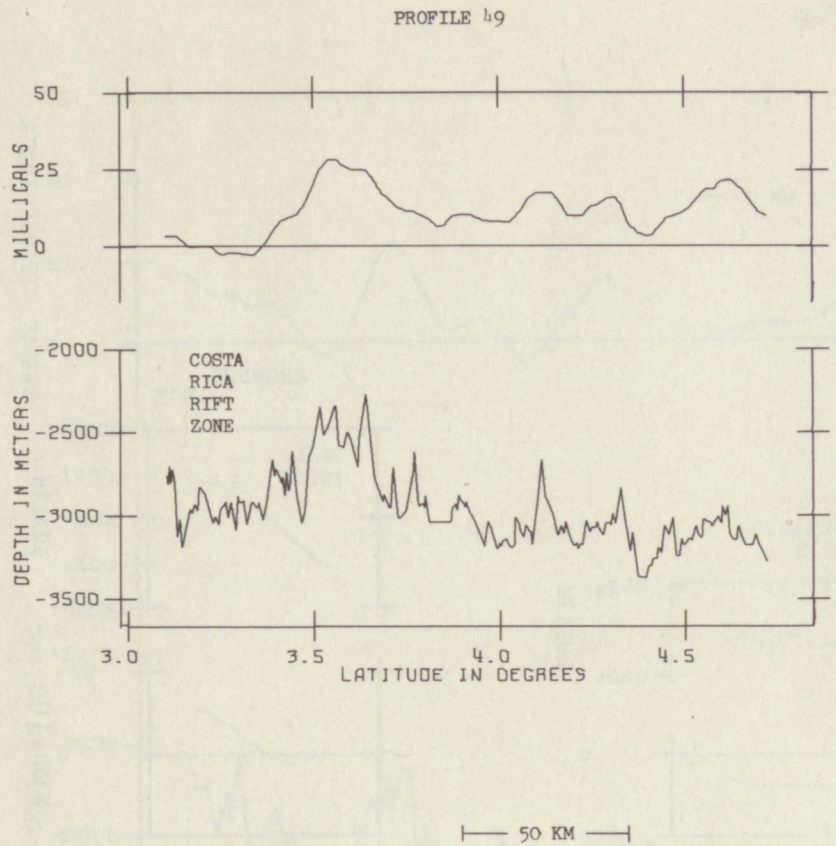
PROFILE 49
50
25
0
MILLIGALS
-2000
-2500
-3000
-3500
DEPTH IN METERS
COSTA
RICA
RIFT
ZONE
3.0
3.5
4.0
4.5
LATITUDE IN DEGREES
50 KM

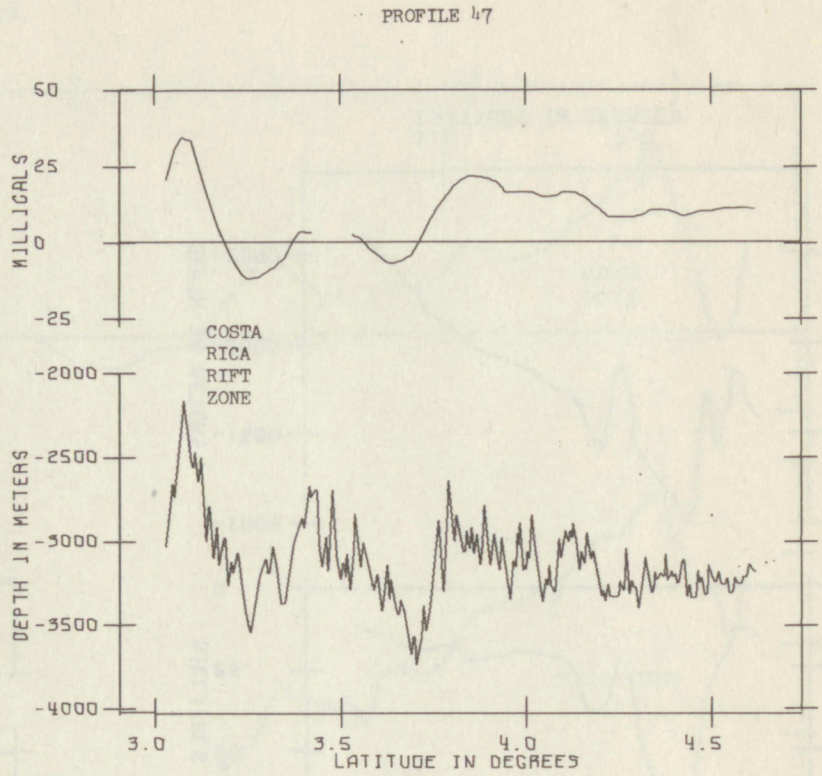
PROFILE 47
50
25
0
-25
MILLIGALS
-2000
-2500
-3000
-3500
-4000
DEPTH IN METERS
COSTA
RICA
RIFT
ZONE
3.0
3.5
4.0
4.5
LATITUDE IN DEGREES

PROFILE 18

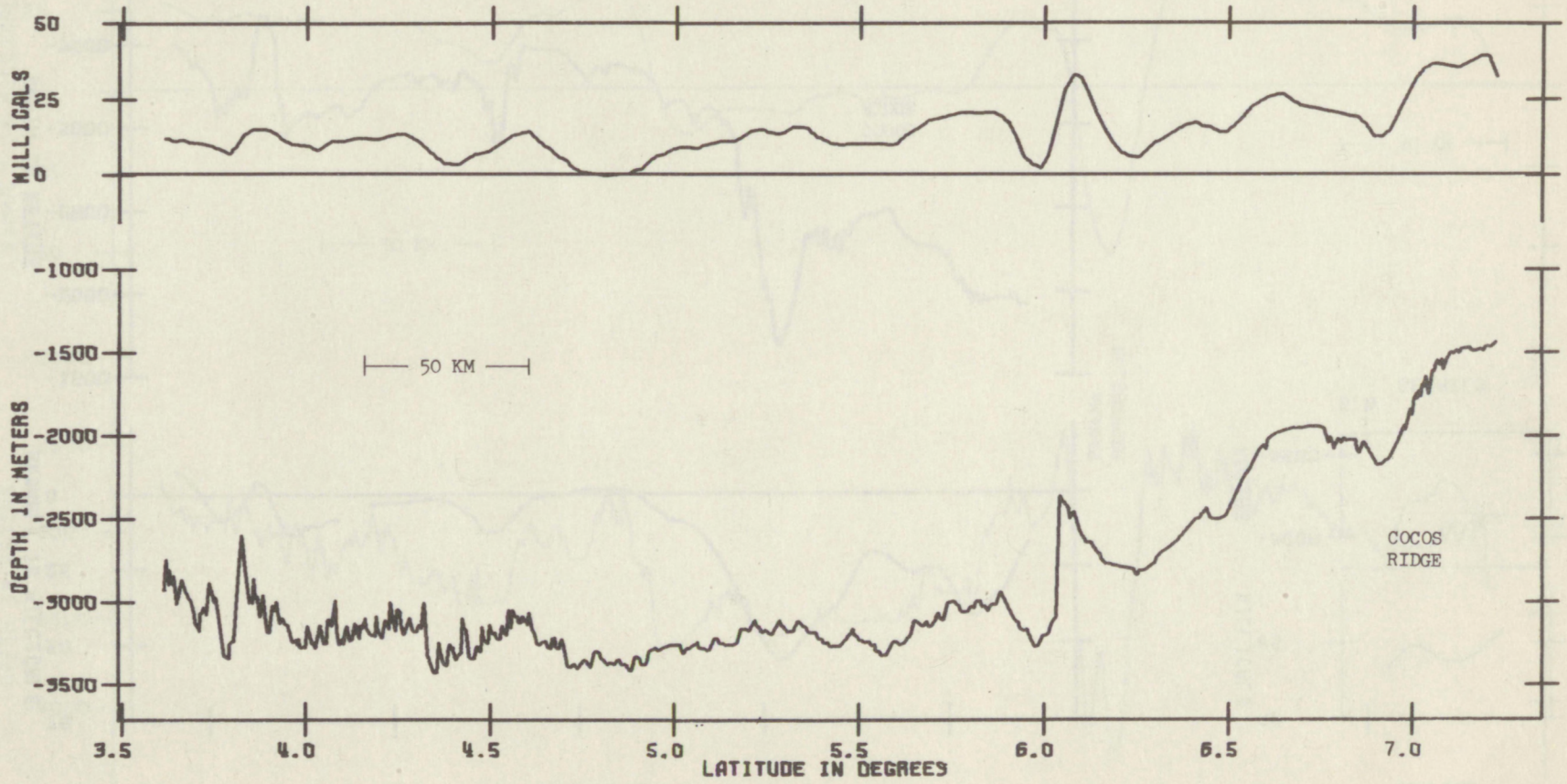
50
25
0
MILLIGALS
-1000
-1500
-2000
-2500
-3000
-3500
DEPTH IN METERS
50 KM
COCOS
RIDGE
3.5
4.0
4.5
5.0
5.5
6.0
6.5
7.0
LATITUDE IN DEGREES

PROFILE 20

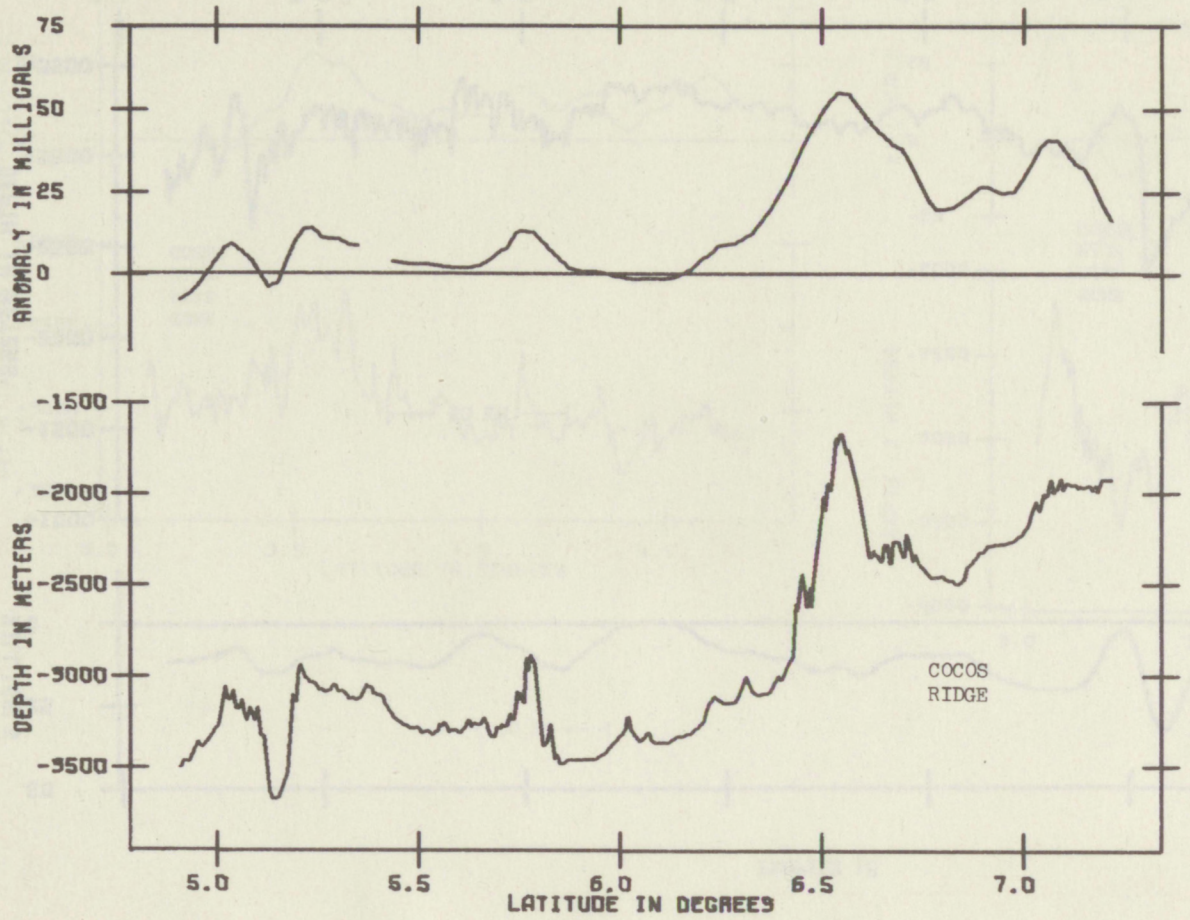

PROFILE 4

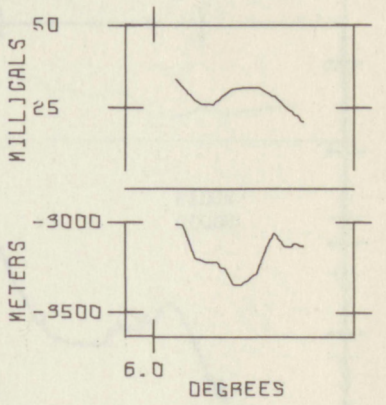

50 KM

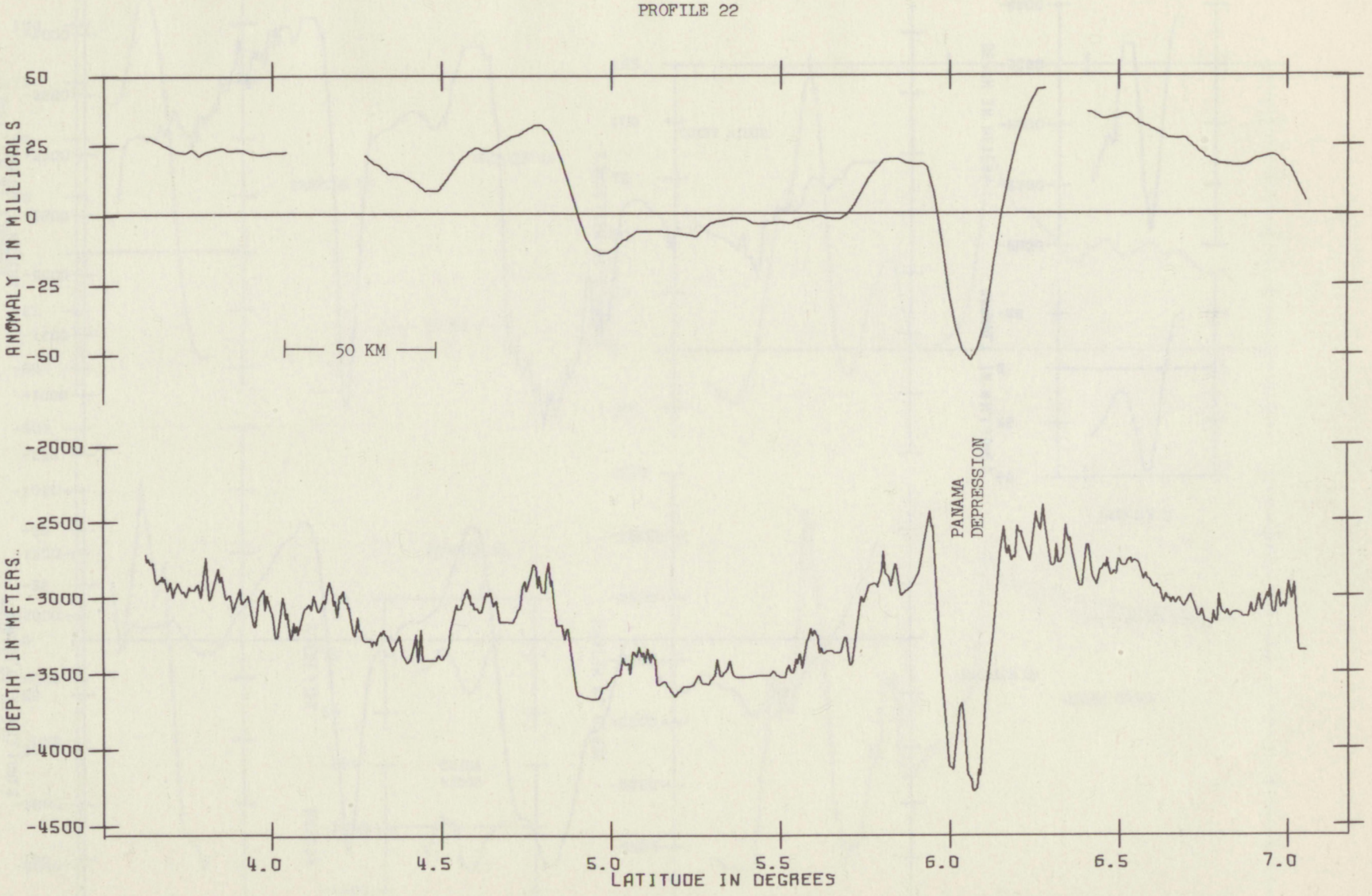
PROFILE 22
50
25
0
-25
-50
ANOMALY IN MILLIGALS
50 KM
-2000
-2500
-3000
-3500
-4000
-4500
DEPTH IN METERS
PANAMA
DEPRESSION
4.0
4.5
5.0
5.5
6.0
6.5
7.0
LATITUDE IN DEGREES

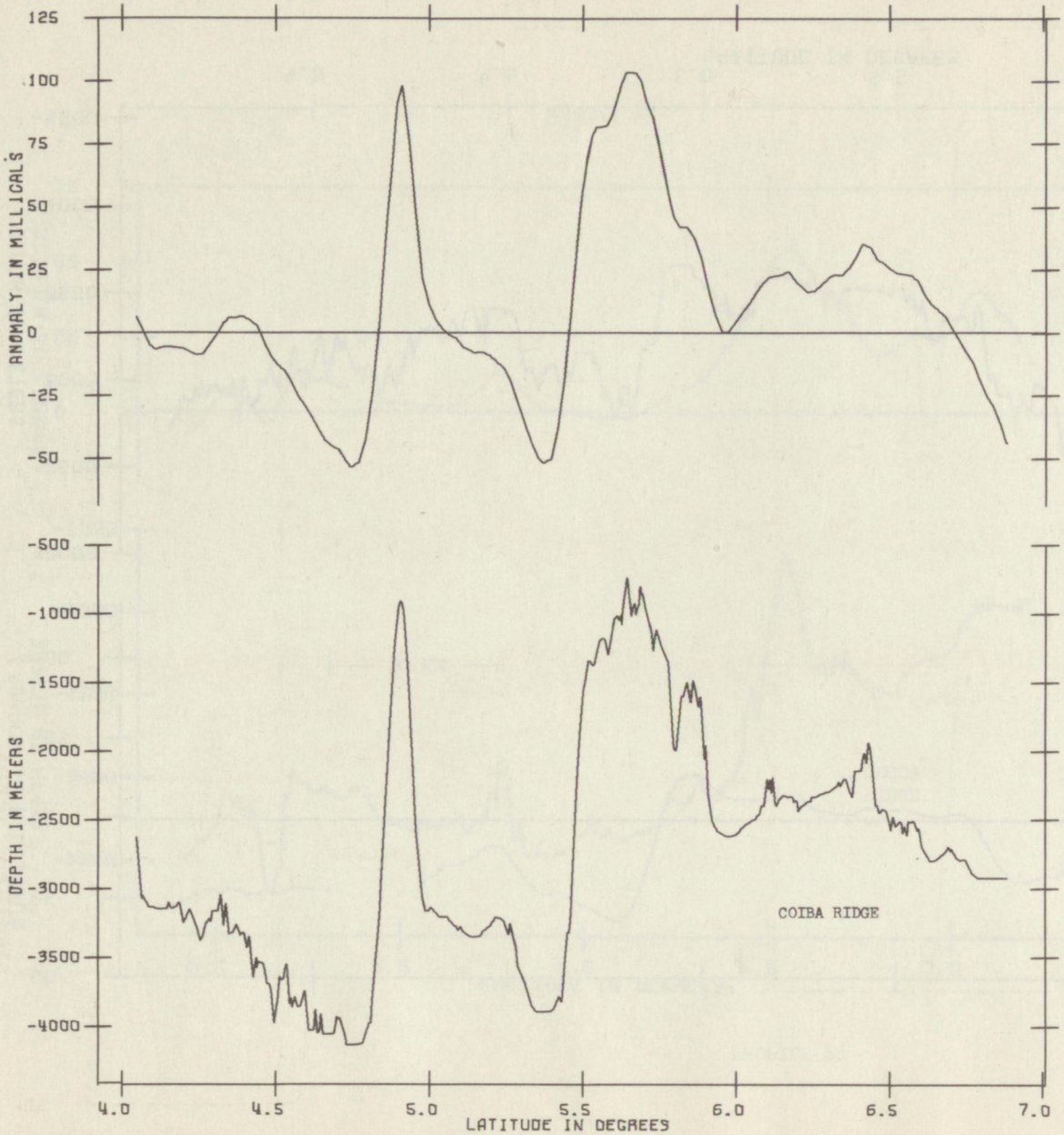

PROFILE 24

50 KM

PROFILE 8

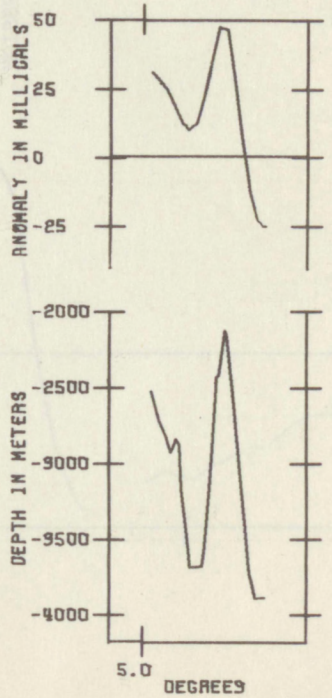

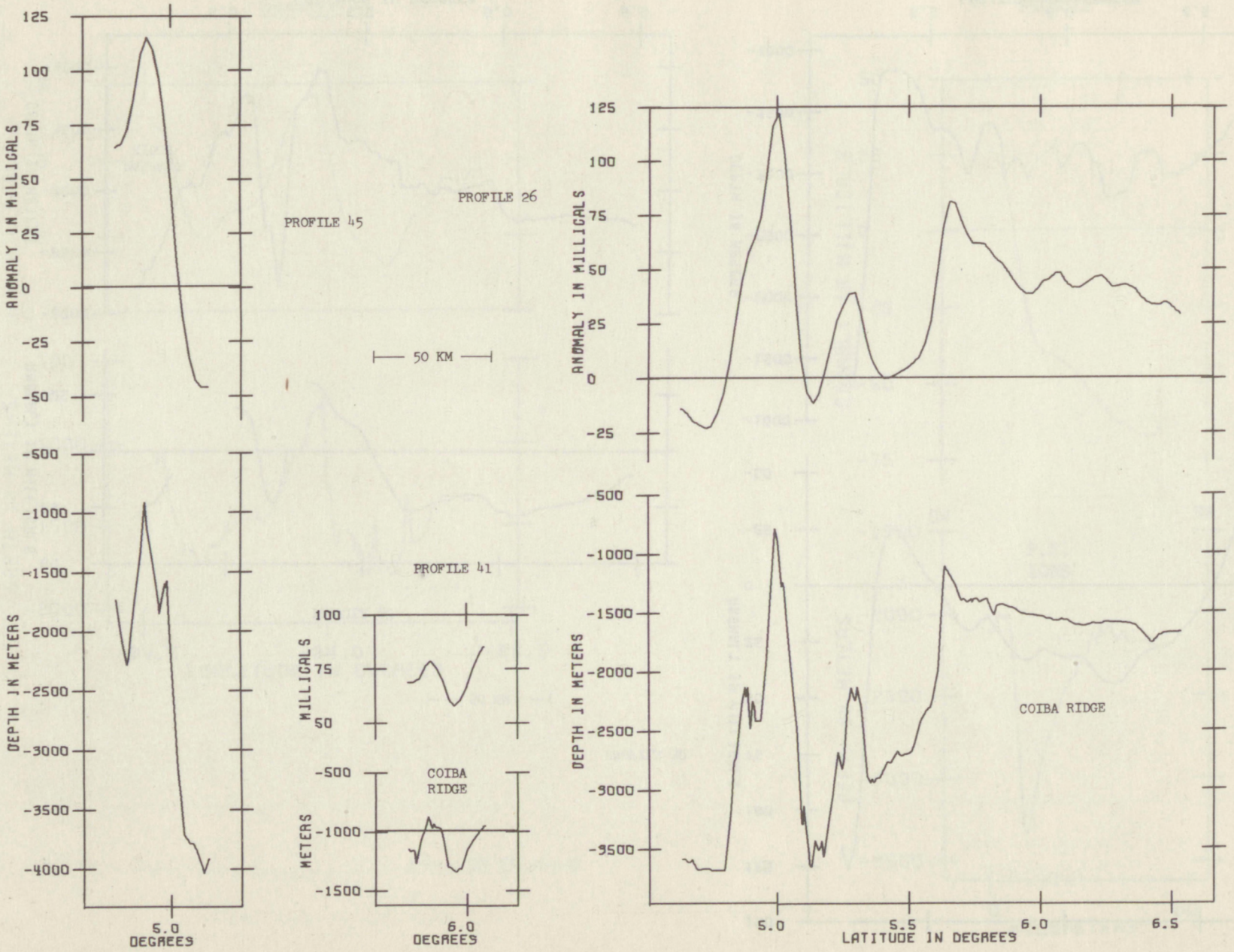
125
100
75
50
25
0
-25
-50
ANOMALY IN MILLIGALS
PROFILE 45
PROFILE 26
50 KM
-500
-1000
-1500
-2000
-2500
-3000
-3500
-4000
DEPTH IN METERS
5.0
DEGREES
PROFILE 41
100
75
50
MILLIGALS
-500
-1000
-1500
METERS
COIBA
RIDGE
6.0
DEGREES
125
100
75
50
25
0
-25
ANOMALY IN MILLIGALS
-500
-1000
-1500
-2000
-2500
-3000
-3500
DEPTH IN METERS
COIBA RIDGE
5.0
5.5
6.0
6.5
LATITUDE IN DEGREES

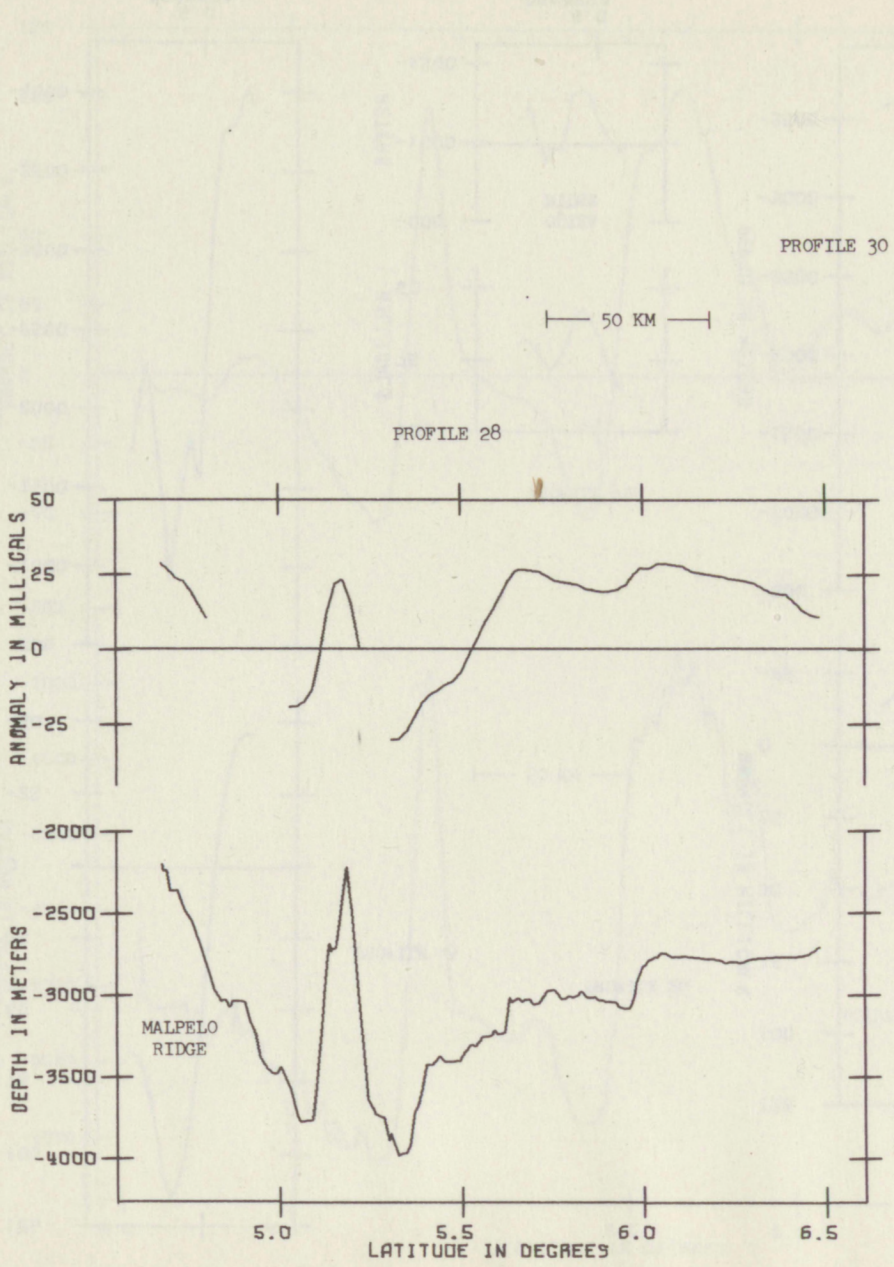
PROFILE 28
50 KM
ANOMALY IN MILLIGALS
50
25
0
-25
DEPTH IN METERS
-2000
-2500
-3000
-3500
-4000
MALPELO
RIDGE
5.0
5.5
6.0
6.5
LATITUDE IN DEGREES

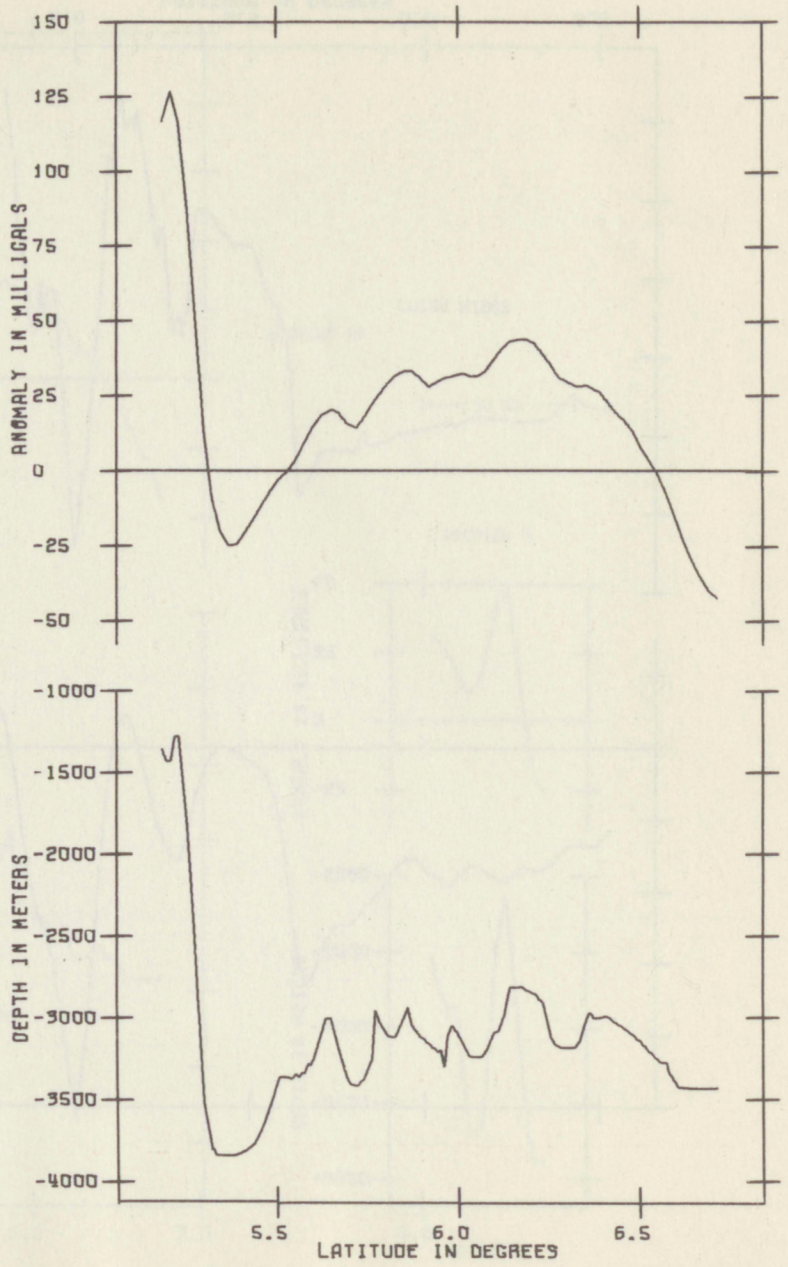
PROFILE 30
ANOMALY IN MILLIGALS
150
125
100
75
50
25
0
-25
-50
DEPTH IN METERS
-1000
-1500
-2000
-2500
-3000
-3500
-4000
5.5
6.0
6.5
LATITUDE IN DEGREES

PROFILE 62

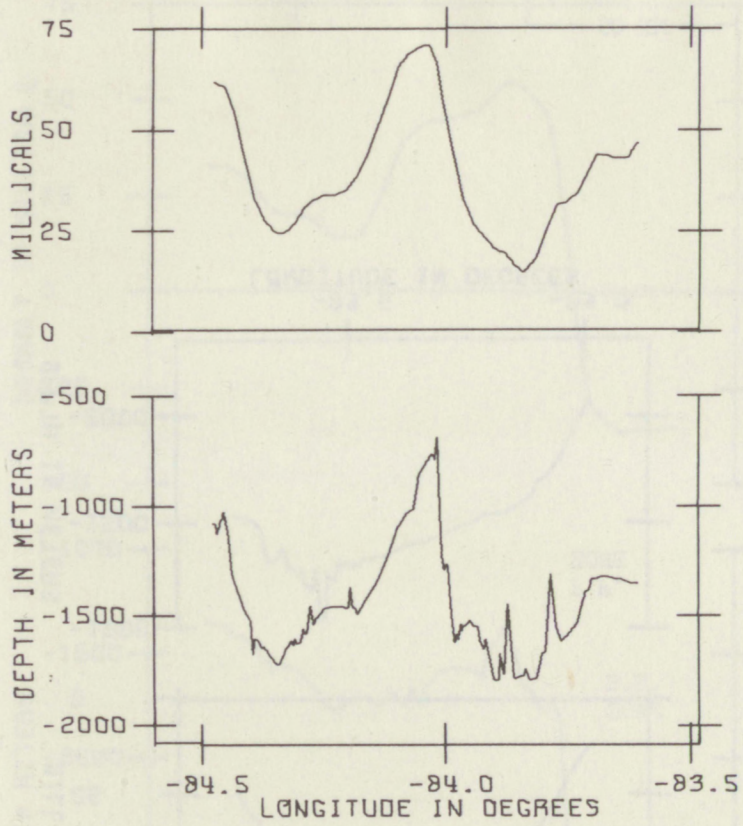

50 KM

PROFILE 55

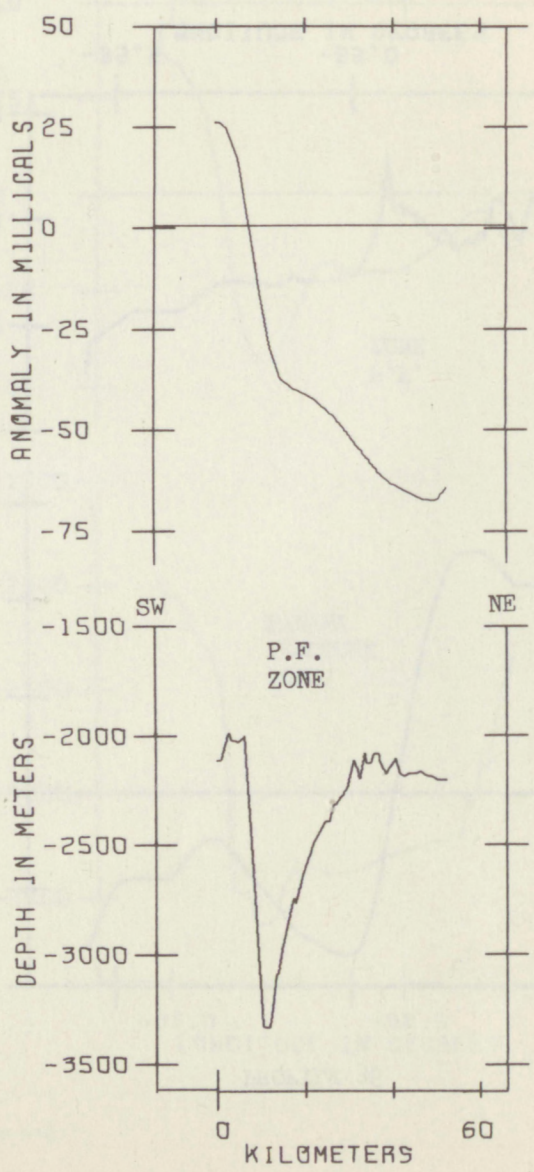

PROFILE 34

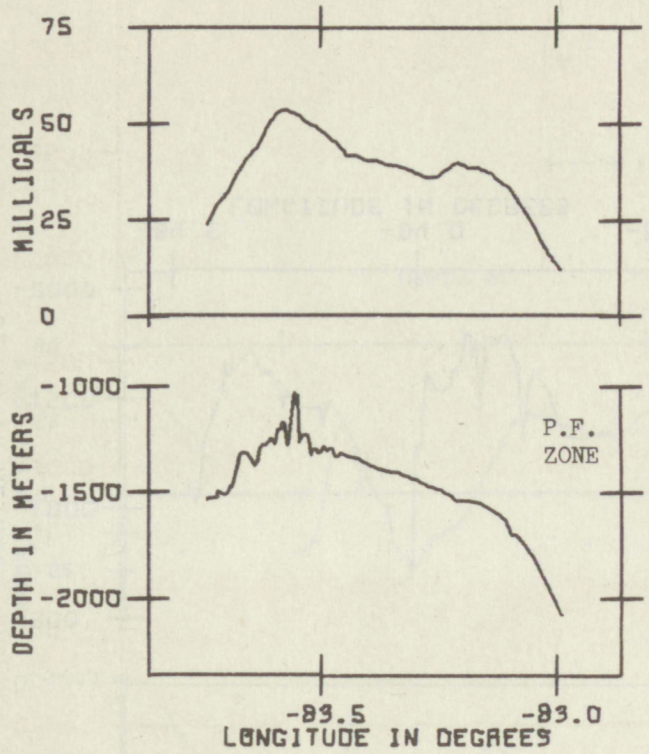

50 KM

PROFILE 36

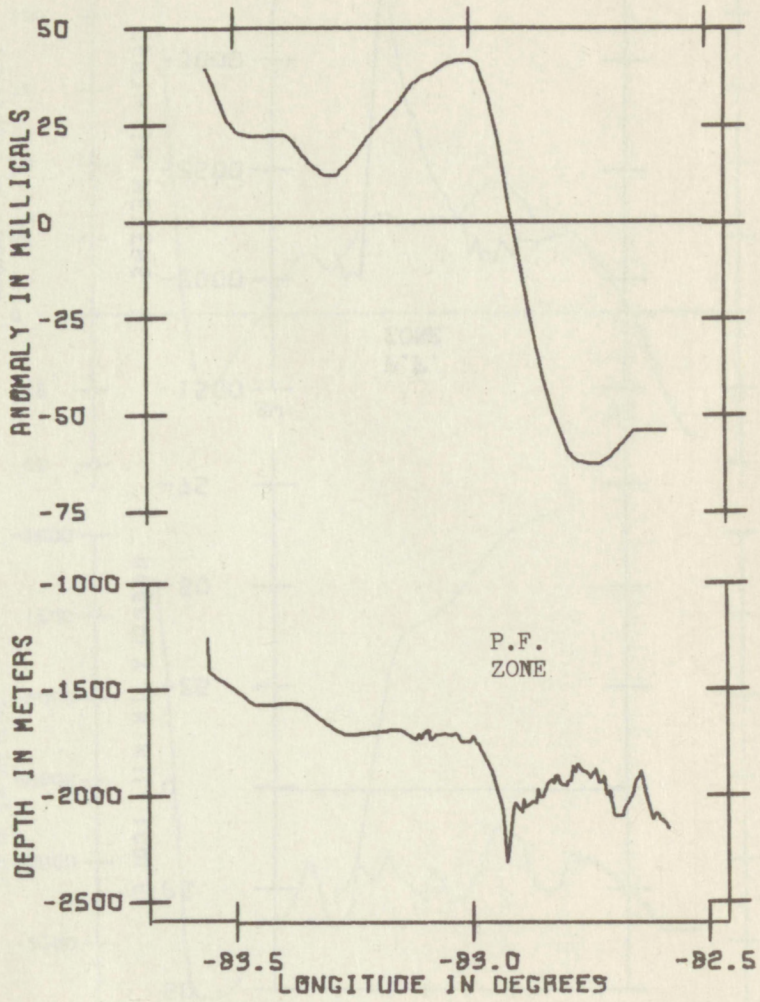

PROFILE 38

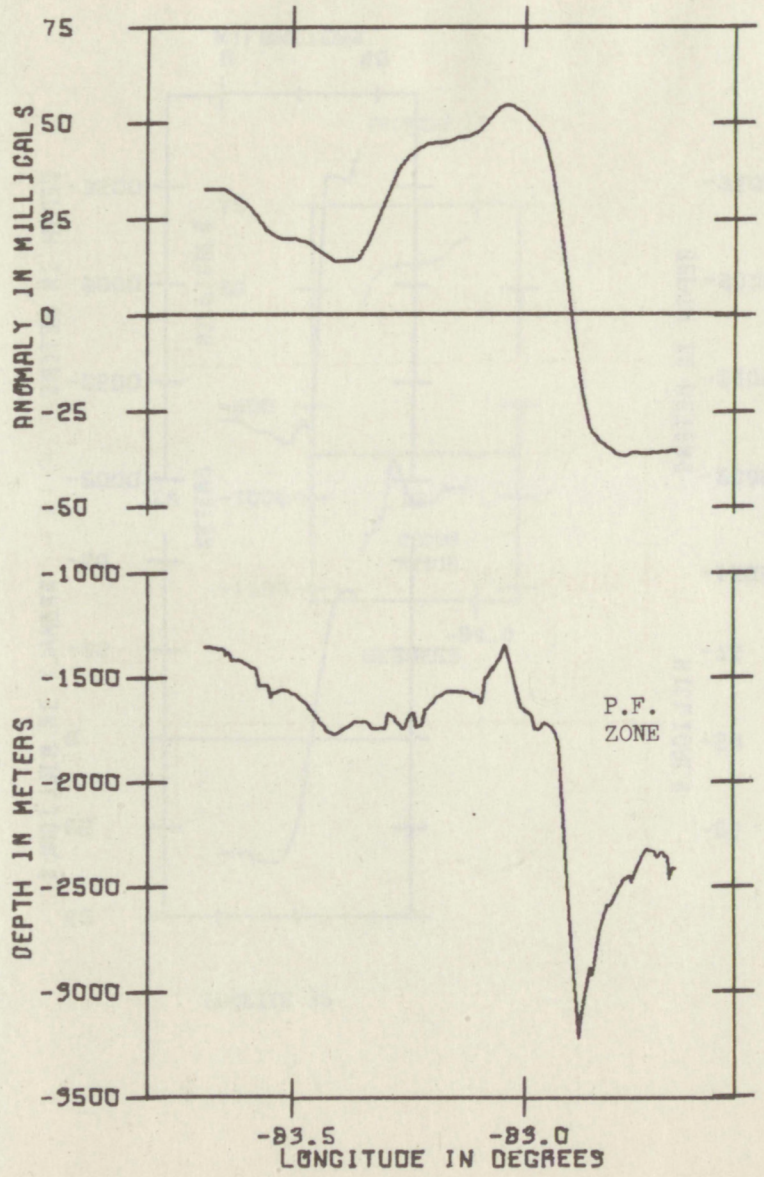

PROFILE 54

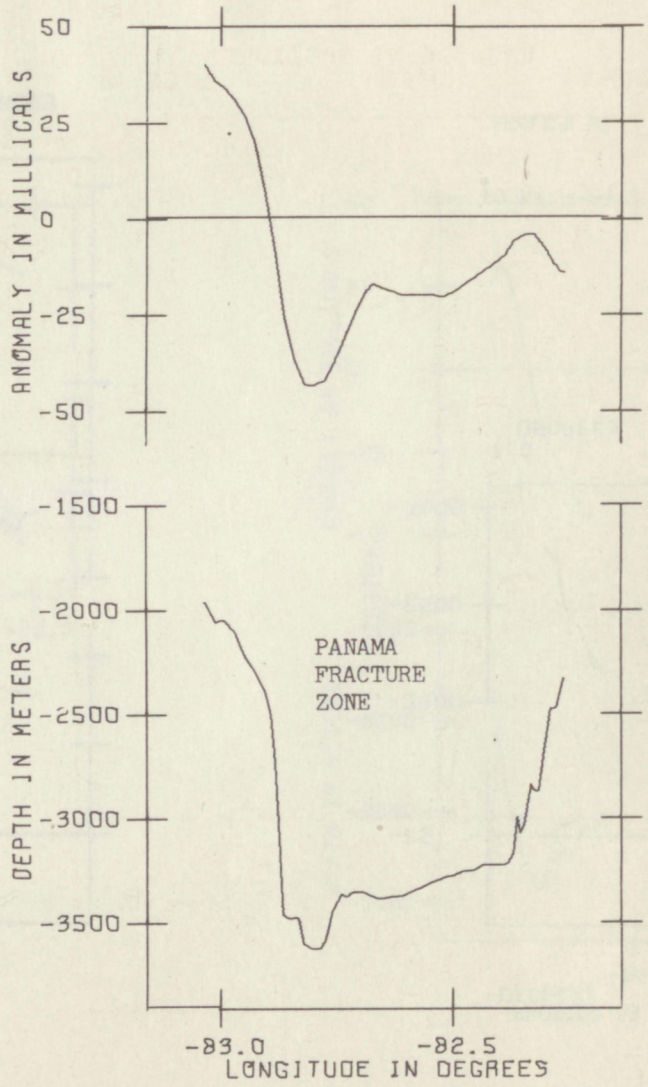

50 KM

PROFILE 32

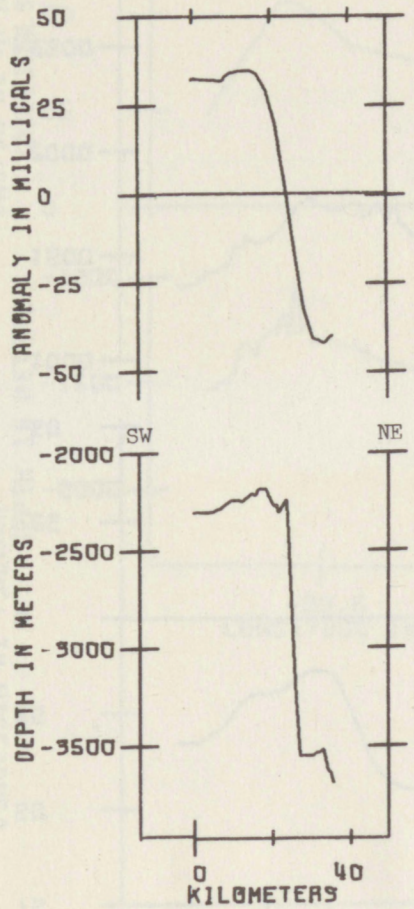

PROFILE 33

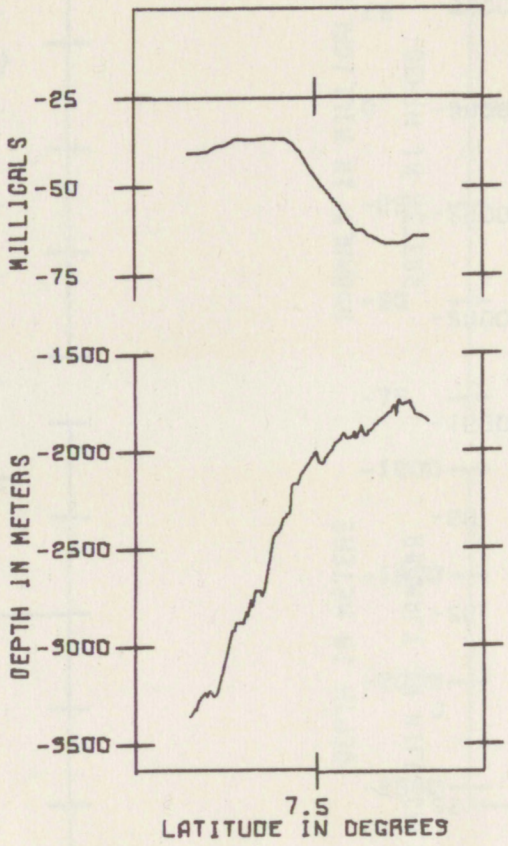

PROFILE 53

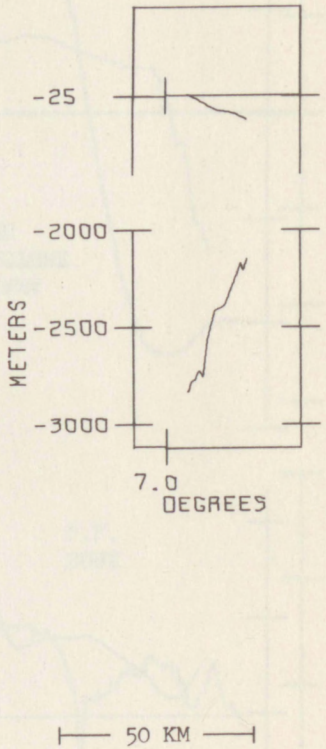

PROFILE 15

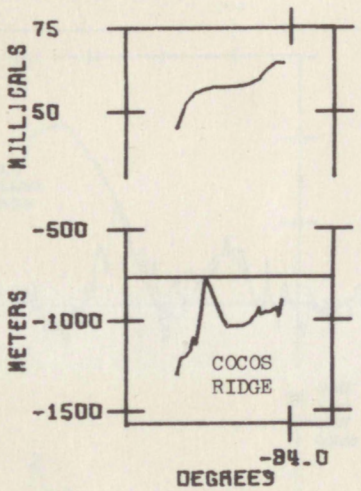

PROFILE 19

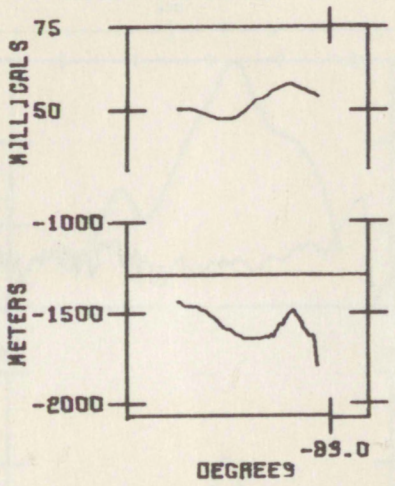

50 KM

PROFILE 23

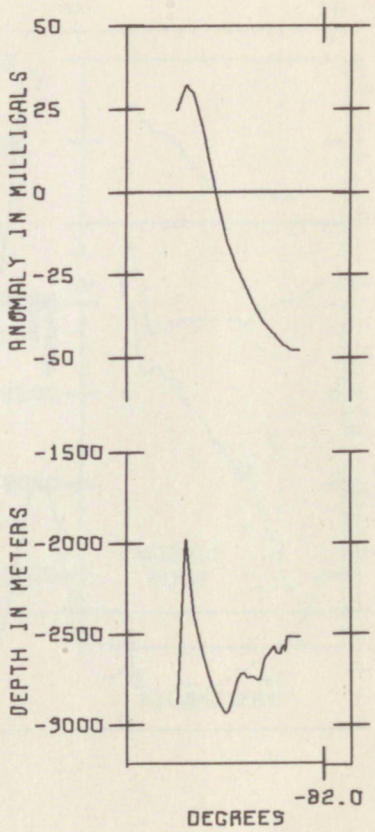

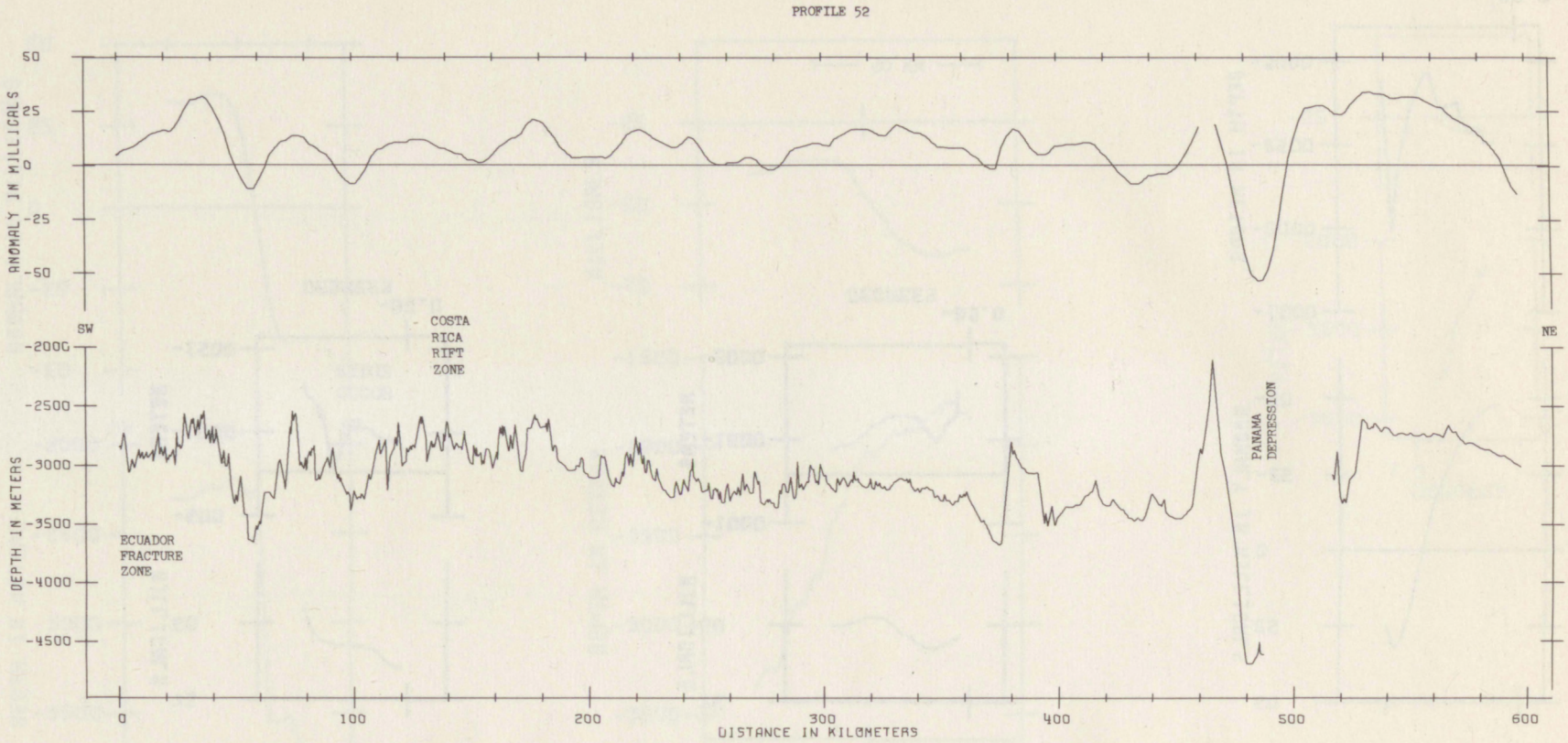
PROFILE 52
50
25
0
-25
-50
ANOMALY IN MILLIGALS
SW
NE
COSTA
RICA
RIFT
ZONE
PANAMA
DEPRESSION
ECUADOR
FRACTURE
ZONE
-2000
-2500
-3000
-3500
-4000
-4500
DEPTH IN METERS
0
100
200
300
400
500
600
DISTANCE IN KILOMETERS

PROFILE 25

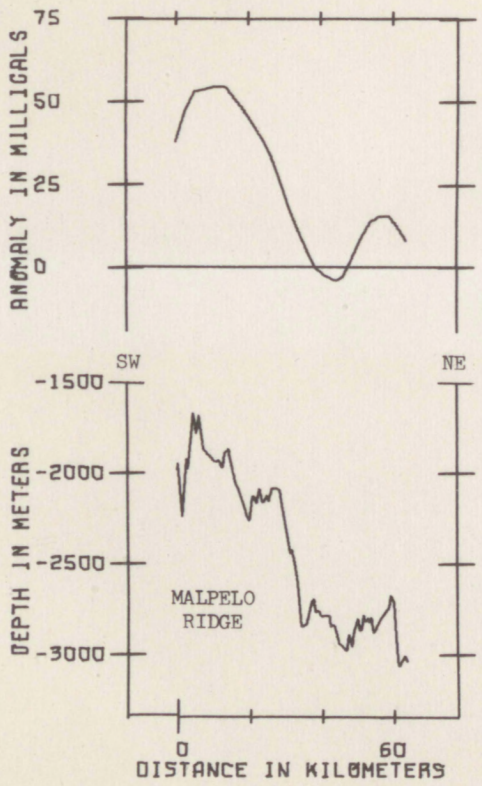

PROFILE 12

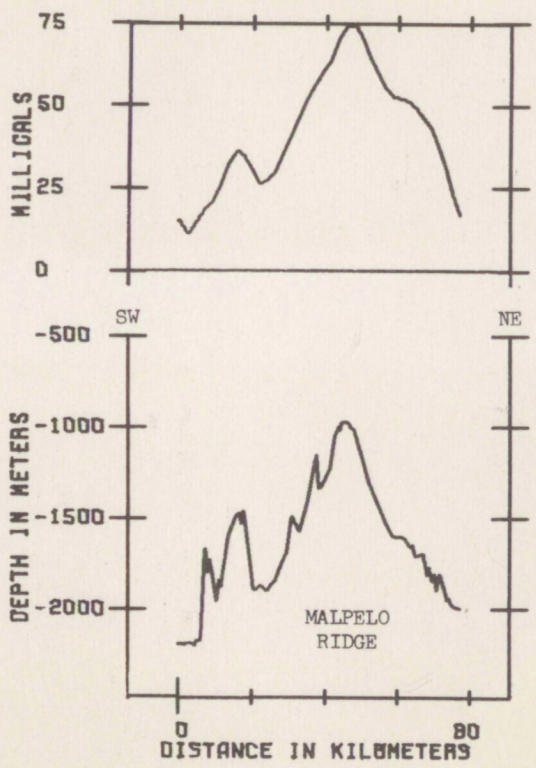

PROFILE 29

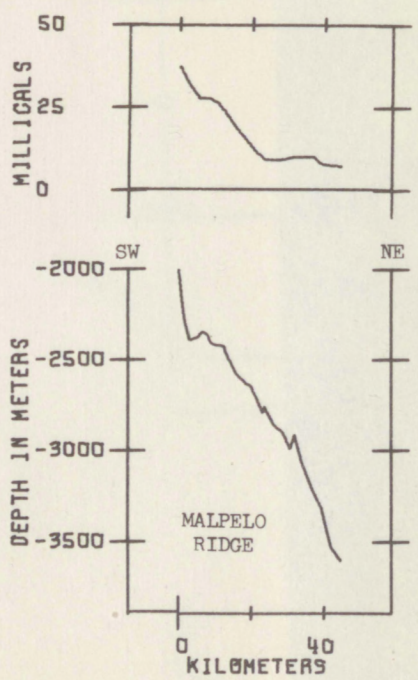

GPO 837-327

COSTA RICA

PANAMA

9°N

8°

7°

6°

5°

4°

3°

2°N

85°W

84°

83°

82°

81°

80W

60 58 34 56 35 36 37 38 55 33 15 19 54 39 23 1 32 31 2 20 27 3 24 40 4 14 16 5 41 6 42 26 28 30 43 22 7 44 8 45 9 18 10 29 50 46 11 49 25 12 13B 13A 17 47 21 51 48 52

PANAMA FRACTURE ZONE

COSTA RICA RIFT ZONE

ECUADOR FRACTURE ZONE

PANAMA DEPRESSION

ECUADOR DEPRESSION

GPO 831-314

PLATE 1